New description of "*Megaptera*" *hubachi* Dathe, 1983 based on the holotype skeleton held in the Museum für Naturkunde, Berlin

Michelangelo Bisconti[1]

SUMMARY: A new focus on "Megaptera" hubachi *revealed that this balaenopterid from the Chilean Pliocene does not belong to* Megaptera *and needs a new generic name. Comparative and phylogenetic analyses suggest that it belongs to a radiation including most of post-Parabalaenopterinae balaenopterids but it was impossible to find its sister group. The analysis of feeding-related traits (shape of glenoid fossa of the squamosal, morphology of the dentary, shape of the frontal) showed that* "M." hubachi *was able to perform a muscular-assisted intermittent ram feeding which was lacking the mechanism to save and release mechanical energy typical of living balaenopterids. The comparative analysis of the dentary suggests that* "M." hubachi *had numerous ventral throat grooves resembling the living humpbacks and rorquals. The map of the presence/absence of the analysed feeding-related traits on the balaenopterid phylogeny allowed to preliminarily infer aspects of the evolution of the feeding behavior of Balaenopteridae.*
***Key words**:* Balaenoptera*, Balaenopteridae, Chile, Feeding behavior,* Megaptera*, Phylogeny.*

RIASSUNTO: Un nuovo esame di *"Megaptera" hubachi* ha rivelato che questo balenotteride cileno pliocenico non appartiene al genere *Megaptera* e deve essere assegnato ad un nuovo genere di misticete. Analisi comparative e filogenetiche suggeriscono che *"M." hubachi* appartenga ad una radiazione che include tutti i balenotteridi apparsi dopo Parabalaenopterinae. Comunque è stato impossibile individuarne il sister group. L'analisi dei caratteri legati all'alimentazione (forma della fossa glenoidea dello squamoso, morfologia della mandibola, forma del frontale) ha mostrato che *"M." hubachi* era in grado di realizzare un meccanismo di alimentazione del tipo intermittent ram feeding (tipico degli attuali balenotteridi) ma con una maggior partecipazione della componente muscolare. L'analisi comparata della mandibola suggerisce che *"M." hubachi* avesse numerose pieghe golari similmente a quanto si osserva nelle attuali balenottere e megattere. La mappa dell'assenza/presenza dei caratteri legati all'alimentazione sulla filogenesi dei balenotteridi ha consentito, in via preliminare, di inferire aspetti dell'evoluzione dei comportamenti alimentari di Balaenopteridae.
Parole chiave: *Balaenoptera*, Balaenopteridae, Cile, Comportamento alimentare, Filogenesi, *Megaptera*.

Introduction

Despite recent investigations and taxonomic updates (Bisconti, 2010a, 2007a,b; Bosselaers, Post, 2010; Deméré *et al.*, 2005), the diversity and phylogenetic relationships of fossil balaenopterid mysticetes (which include rorqual and humpback whales) are still scarcely known. Being the most successful family of living baleen whales, balaenopterids have a fossil history that allows to infer a Late Miocene origin of the family (Bisconti, 2010a; Zeigler *et al.*, 1997) and a subsequent diversification during the latest Miocene and the Pliocene with the origin of several genus-rank taxa and widespread diffusion all over the world oceans (Bisconti, 2010b). Deméré *et al.* (2005) pointed out that many of the balaenopterid taxa established in the 19th century are in critical need of revision and provided a first assessment of the validity of a number of genera described by early

1. Museo di Storia Naturale del Mediterraneo, Via Roma 234, 57100, Livorno. E-mail: zoologia.museo@provincia.livorno.it

authors. Bisconti (2009, 2008, 2007b) reviewed the taxonomy of some Italian controversial specimens and, together with Deméré (1986) and Bisconti (2003), rejected the logical basis of the foundation of the chronospecies *Balaenoptera acutorostrata cuvieri* supported by Caretto (1970); in this way it is now newly open the field for new taxonomic studies of Italian Pliocene balaenopterids described in the 19th and early 20th century.

Starting from the seminal work of Zeigler *et al*. (1997), a number of phylogenetic analyses of balaenopterids have been published resulting into three different main results. Zeigler *et al*. (1997) suggested that Balaenopteridae Gray, 1864 is formed by three subfamilies: Parabalaenopterinae (including Miocene species; see also Bisconti, 2010a), Megapterinae (including the humpback whale *Megaptera novaeangliae* (Borowski, 1781)), and Balaenopterinae (including the rorqual whales of the genus *Balaenoptera*). Bisconti (2010a, 2007a,b) substantially supported this view based on a comprehensive cladistic analysis of mysticetes. In their morphology-based analysis, Deméré *et al*. (2005) were unable to find a monophyletic Balaenopterinae; their study resulted into a clade including *Balaenoptera edeni* Anderson, 1879, *B. borealis* Lesson, 1828, and *B. acutorostrata* Lacépède, 1804; a clade including *B. musculus* (Linnaeus, 1758), *B. davidsonii* (Cope, 1872), and *Parabalaenoptera baulinensis* Zeigler *et al*., 1997 that shares a common ancestry with the previous clade; they found also a third clade including "*Megaptera" hubachi* Dathe, 1983, *Balaenoptera siberi* Pilleri, 1989, and *B. physalus* (Linnaeus, 1758). *Megaptera novaeangliae* was found to be basal to these branches and "*Megaptera" miocaena* Kellogg, 1922 was found to be the sister group of the first two clades. Deméré *et al*. (2008) published a different cladistic analysis based on a higher number of morphological characters and molecular data; such an analysis, as far as Balaenopteridae is concerned, resulted in an unresolved polytomy in which only a few relationships were supported (such as *Balaenoptera edeni* + *B. borealis*).

The problem of the phylogenetic relationships of balaenopterid mysticetes is further complicated by the lack of genetic support (at the moment) for a monophyletic Balaenopteridae as the gray whale *Eschrichtius robustus* Lilljeborg, 1861 is genetically nested within *Balaenoptera*; in this sense, molecular biologists found that neither Balaenopteridae nor *Balaenoptera* are monophyletic (e.g., Rychel *et al*., 2004), a result which is in sharp contrast to morphology-based studies (Bisconti, 2010a; Hampe, Baszio, 2010; Deméré *et al*., 2005).

Phylogenetic works on balaenopterids including the fossil record have mainly focused on taxa from the northern hemisphere but published reports documented the presence of interesting specimens from New Zealand, Peru and Chile. Although it is well known that fossil deposits in South America include high numbers of well preserved balaenopterid skeletons (e.g., Brand *et al*., 2004), only a few studies reported about the morphological diversity of such a rich evidence. Among them, the works by Pilleri (1989) and Dathe (1983) respectively on *Balaenoptera siberi* and "*Megaptera" hubachi* are the most representative as far as anatomy and taxonomy are concerned. Brief reviews of these taxa have been provided by Deméré *et al*. (2005).

The type locality of *Balaenoptera siberi* is Aguada de Lomas in the Sacaco Basin (southern Peru); there, Messinian levels (around 6 Ma) of Pisco Formation outcrop. The type locality of "*Megaptera" hubachi* is Bahia de Guayacan (northern Chile; Fig. 1) and the uncertain stratigraphy of the type specimen has to relies on the information provided by Dathe (1983) who stated that the specimen is from Pliocene marine sandstone. According to Deméré *et al*. (2005) the estimated age of the holotype skeleton should be Piacenzian (around 3 Ma).

These two South American balaenopterid taxa are represented by almost complete skeletons in which most of the informative characters are preserved and can be used for detailed descriptions and phylogenetic analysis. Although the descriptions provided by Pilleri (1989) and Dathe (1983) were detailed enough to warrant complete representations of the species, in the last few years different authors specifically focused on specialized traits related to feeding behavior and hearing and these were only superficially reported in the original descriptions. For this reason, a new study of the specimens and a new assessment of their phylogenetic relationships under a morphology-based cladistic approach promise to bring to light previously undescribed or underrepresented features of these South American species.

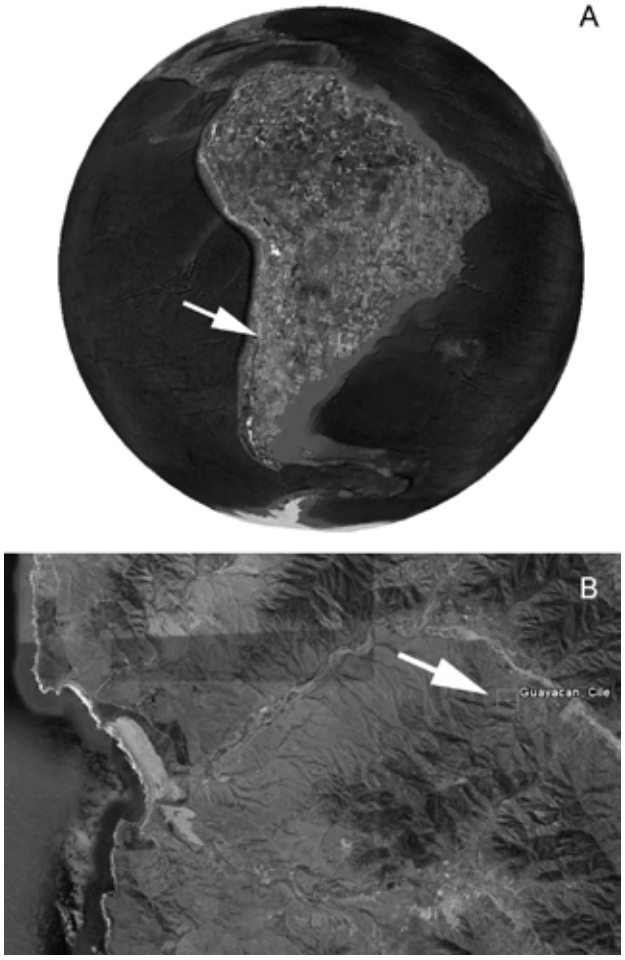

Fig. 1 - Type locality of "*Megaptera" hubachi* Dathe, 1983. A, South America with indicated the approximate position of the type locality. B, Guayacan, Chile. Type locality.
Fig. 1 - Località-tipo di "Megaptera" hubachi *Dathe, 1983. A, America meridionale con indicata la posizione approssimativa della località-tipo. B, Località-tipo: Guayacan, Chile.*

In this paper, a new study of the holotype skeleton of "*Megaptera" hubachi* is presented together with an osteology-based analysis of its phylogenetic relationships. The skeleton is compared to the known record of living and fossil balaenopterid taxa and its relationships should help to reconstruct part of the evolutionary history of the feeding mechanisms of Balaenopteridae and should also allow to have a preliminary overview of the paleobiogeography of this family.

Morphological observations on "*Megaptera*" *hubachi*

The specimen was studied during its temporary exhibition at the Museum für Naturkunde in Berlin. The earbones were made available for a study outside the exhibition room. The skeleton includes reconstructed portions that have been individuated in the figures of the present paper.

Material

Partial skeleton MB.Ma. 28570 held by the Museum für Naturkunde in Berlin (Figs. 2,3); the skeleton includes a partial skull and dentaries together with parts of the axial skeleton and limb elements.

Description

The specimen consists in an almost complete skeleton which is approx. 6 m in length. The right humerus, radius and ulna are lacking; the neural processes of the cervical and lumbar vertebrae are missing; 14 caudal vertebrae are missing and have been reconstructed; many of the fingers are lacking; the anterior portions of the dentaries and the lateral borders of the maxillae are broken;

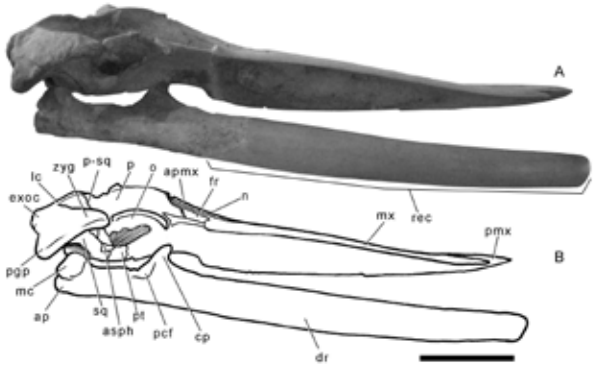

Fig. 2 - "*Megaptera" hubachi*, skull in right lateral view. A, picture; B, schematic representation. Scale bar equals 300 mm Explanation of abbreviations: ap, angular process of the dentary; apmx, ascending process of the maxilla; asph, alisphenoid; cp, coronoid process of dentary; dr, dentary ramus; exoc, exoccipital; fr, fontal; lc, lambdoid crest; mc, mandibular condyle; mx, maxilla; n, nasal; o, orbit; p, parietal; pcf, postcoronoid fossa of the dentary; pgp, postglenoid process of the squamosal; pmx, premaxilla; pt, pterygoid; p-sq, parietal-squamosal suture; rec, reconstructed portion of the dentary; sq, squamosal; zyg, zygomatic process of the squamosal.
Fig. 2 - "Megaptera" hubachi*, cranio in norma laterale destra. A, foto; B, rappresentazione schematica. La barra equivale a 300 mm. Legenda: ap, processo angolare della mandibola; apmx, processo ascendente del mascellare; asph, alisfenoide; cp, processo coronoideo della mandibola; dr, ramo mandibolare; exoc, esoccipitale; fr, frontale; lc, cresta lambdoidea; mc, condilo della mandibola; mx, mascellare;n, nasale; o, orbita; p, parietale; pcf, fossa postcoronoidea della mandibola; pgp, processo postglenoideo dello squamoso; pmx, premascellare; pt, pterigoideo; rec, parte ricostruita del ramo mandibolare; p-sq, sutura tra parietale e squamoso; sq, squamoso; zyg, processo zigomatico dello squamoso.*

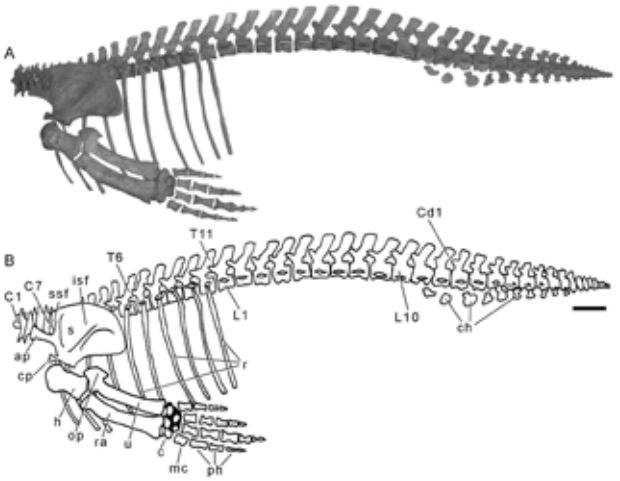

Fig. 3 - *"Megaptera" hubachi*, postcranial skeleton in left lateral view. A, picture; B, schematic representation. Scale bar equals 300 mm. Explanation of abbreviations: ap, acromion process of scapula; c, carpal bones; C1 and C7, 1st and 7th cervical vertebrae; Cd1, 1st caudal vertebra; ch, chevron; cp, coracoid process of scapula; h, humerus; isf, infraspinous fossa of scapula; L1 and L10, 1st and 10th lumbar vertebrae; mc, metacarpal bones; op, olecranon process of ulna; ph, phalanges; r, ribs; ra, radius; s, scapula; ssf, supraspinous fossa of scapula; T1 and T11, 1st and 11th thoracic vertebrae; u, ulna.

Fig. 3 - "Megaptera" hubachi, *scheletro postcraniale in norma laterale sinistra. A, foto; B, rappresentazione schematica. La barra equivale a 300 mm. Legenda: ap, processo acromiale della scapola; c, ossa carpali; C1 e C7, prima e settima vertebra cervicale; Cd1, prima vertebra caudale; ch, chevron; cp, processo coracoideo della scapola; h, omero; isf, fossa infraspinosa della scapola; L1 e L10, prima e decima vertebra lombare; mc, ossa metacarpali; op, processo olecranico dell'ulna; ph, falangi; r, coste; ra, radio; s, scapola; ssf, fossa supraspinosa della scapola; T6 e T11, sesta e undicesima vertebra toracica; u, ulna.*

jugal and lacrimal are missing. The individual was an adult as the vertebral epyphyses are completely fused with the vertebral bodies. The distal epyphyses of the left radius and ulna are not fused. The following text consists in a description of the skeleton which should be integrated by the reading of Dathe's (1983) paper where all the measurements are presented.

Skull

The premaxilla is flat and long anteriorly to the narial fossa; its lateral border parallels the medial border of the maxilla posteriorly up to the vertex. The posterior end of the premaxilla is located in proximity of the posterolateral corner of the nasal.

The maxilla is anteroposteriorly elongated and transversely expanded. The medial border of the maxilla diverges from the longitudinal axis of the skull suggesting that the premaxilla was transversely expanded at its anterior end. Right and left maxilla bear respectively 3 and 4 maxillary foramina. The ascending process of the maxilla is long and projects posteriorly and medially (Figs. 4, 5); its posterior end is rounded. It covers the interorbital region of the frontal which can be observed only as a subtle stripe of bone surrounding the lateral and posterior borders of the ascending processes. In ventral view, the maxillae form a strong ventral keel and show evident grooves for the vasculature of the baleen-bearing tissue that are directed anteroposteriorly and transversely. The suture of maxilla and palatine is posteriorly concave. The infraorbital plate is badly damaged and only a small, featureless portion is preserved on the left side.

The nasal is elongated and bears a dorsomedial keel; the lateral border diverges anteriorly and in the anterior border the anteromedial corner is located more anteriorly than the anterolateral corner (Fig. 8).

The supraorbital process of the frontal is abruptly depressed (Fig. 6) from the interorbital region of the frontal. The supraorbital process is wide and flat; its anterior border is directed laterally and posteriorly; its posterior border is directed laterally and slightly anteriorly. The posterior border bears two round relieves (Fig. 8). The ascending temporal crest is not relieved and cannot be individuated. The orbit is elongated and shows a rounded border on the right side that is more linear on the left side. The antorbital corner is located more medially than the postorbital corner. The postorbital corner bears a short but evident articular facet for the zygomatic process of the squamosal. The interorbital region of the frontal includes the posteromedial elements of the rostrum which obliterate it almost completely (Fig. 4). In ventral view, the medial location of the optical channel is in the posterior-most part of the supraorbital process of the frontal; the optical channel is anteriorly bordered by a crest which is posteriorly concave. It widens more distally as the crest becomes lower up to disappear at a short distance from the orbit.

The interparietal cannot be observed. It is probably absent (Fig. 4).

Jugal and lacrimal are missing.

The parietal squama is anteriorly developed

on the depression of the supraorbital process of the frontal and is interdigitated with the ascending process of the maxilla up to around nasal mid-length (Fig. 5). The parietal does not spread over the supraorbital process of the frontal. It is exposed on the vertex for a length of 2.5 cm. The squamosal-parietal sutura is straight and projects dorsally and posteriorly ending anteriorly to the posterior apex of the lambdoid crest. A tubercle is observed at the interface of the sutures of squamosal, parietal and supraoccipital.

The zygomatic process of the squamosal is elongated and has a triangular anterior end which bears a ventral articular facet for the postorbital corner of the supraorbital process of the frontal (Fig. 6). In dorsal view, the zygomatic process is widely divergent from the longitudinal axis of the skull. The postglenoid process of the squamosal projects ventrally and slightly posteriorly. In lateral view, the glenoid fossa of the squamosal is straight and mainly vertical. The posterior wall of the temporal fossa (pertaining to the squamosal) is dorsoventrally short, flat and almost vertical. In its anterior-most part it is dorsally covered by the temporal crest but it is not covered in that part which is posteriorly prolonged to form the posterior apex of the lambdoid crest. The squamosal cleft is present (Fig. 7). It develops starting from the squamosal-alisphenoid suture, projects dorsally and posteriorly paralleling the ventral border of the squamosal, and then turns laterally and ventrally at the level of the lambdoid crest.

The dorsal surface of the supraoccipital is concave. The anterior border of the supraoccipital is located more anteriorly than the anterior end of the zygomatic process of the squamosal and has a concave border. There is no sagittal crest. The attach sites for the neck muscles are well developed and are located on the lateral borders of the supraoccipital (Fig. 8). Two deep parasagittal concavities are located just anterior to the occipital condyles. The temporal crest formed by the dorsal border of the parietal and the lateral border of the supraoccipital overwhelms the temporal fossa anteriorly to the suture point between parietal, squamosal, and supraoccipital; posteriorly to this point, the lateral border of the supraoccipital projects posteriorly nearly parallel to the longitudinal axis of the skull forming a triangular lambdoid crest.

The exoccipital is strongly convex and protrudes more posteriorly than the articular surface of the occipital condyles. The condyles are very rounded and are developed laterally and ventrally to the foramen magnum. The latter shows a dorsal fissure. There are no condyloid foramina. The jugular notch is developed medially to the triangular and ventrally flat descending process of the basioccipital. There is no foramen on the floor of the jugular notch.

Basicranium

The way in which the skeleton was on exhibition in 2009 (the year of the study) prevents a full description of the ventral side of the skull as several metal structures were used to suspend the skull. The hiatus cranicus is transversely wide and has a very round and convex lateral border. This suggests the presence of a periotic with a raised central portion but it is not possible to confirm this based on the preserved earbone fragments.

The descending process of the basioccipital is strongly built and has a gently rounded ventral surface. The external acoustic meatus is transversely elongated but has a short anteroposterior diameter along its whole development. There is no foramen on the floor of the jugular notch. The lateroposterior corner of the exoccipital is located more medially than the postglenoid process and it does not protrude more posteriorly than the squamosal but it protrudes more posteriorly than the occipital condyles.

The earbones are represented by left and right pars cochlearis (MB.Ma. 28570 No. 1 and 4) and some fragments of periotics. The pars cochlearis (Figs. 9, 10) is anteroposteriorly and transversely elongated. The anteroposterior diameter of the right pars cochlearis is 41 mm and its transverse diameter is 38 mm. It seems that the endocranial opening of the facial canal was separated from the internal acoustic meatus. The squared oval window is confluent in the perilymphatic foramen.

The groove under the internal acoustic meatus is absent. Among the fragments there is a part of a triangular anterior process (MB.Ma. 28570 No. 3) which shows an acute apex (Fig. 11). The other fragment is not identified (MB.Ma. 28570 No. 2).

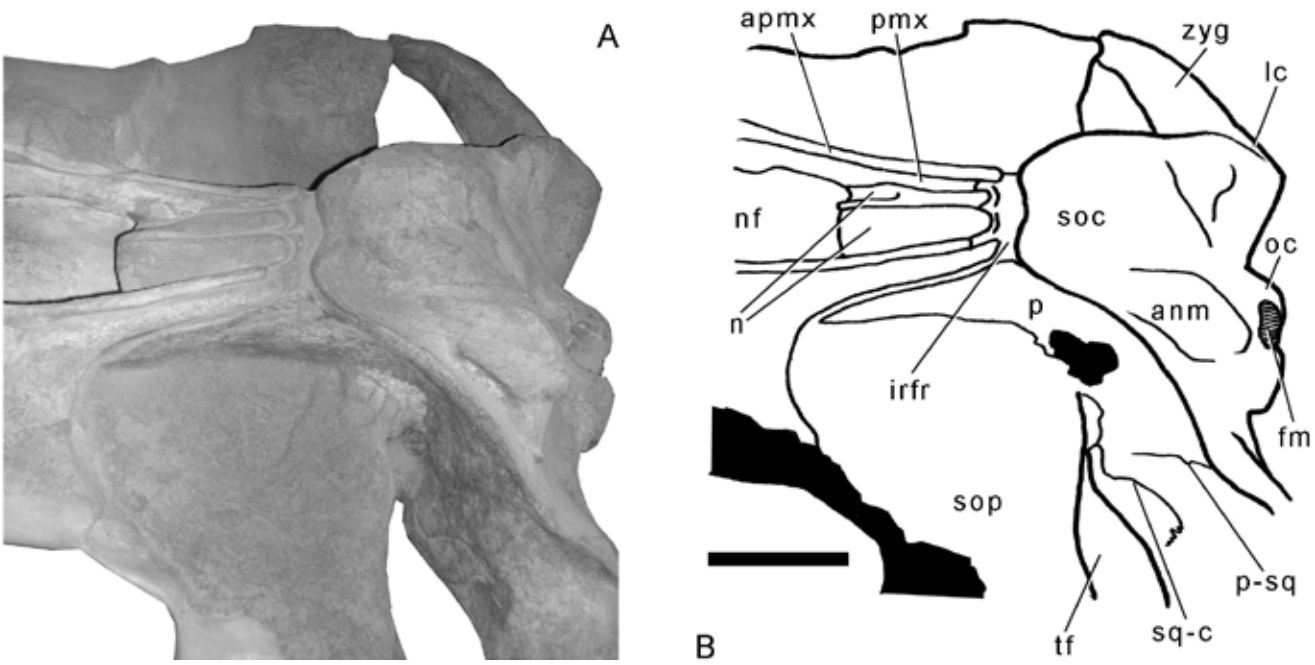

Fig. 4 - *"Megaptera" hubachi*, vertex. A, picture; B, schematic representation. Scale bar equals 100 mm. Explanation of abbreviations: anm, attach site for neck muscles; apmx, ascending process of maxilla; fm, foramen magnum; irfr, interorbital region of frontal; lc, lambdoid crest; n, nasal; nf, narial fossa; oc, occipital condyle; p, parietal; pmx, premaxilla; p-sq, parietal-squamosal suture; soc, supraoccipital; sop, supraorbital process of the frontal; sq-c, squamosal cleft; tf, temporal fossa; zyg, zygomatic process of squamosal.

Fig. 4 - "Megaptera" hubachi*, vertex. A, foto; B, rappresentazione schematica. La barra equivale a 100 mm. Legenda: anm, rilievi per attacco muscoli del collo; apmx, processo ascendente del mascellare; fm, forame magno; irfr, regione interorbitaria del frontale;lc, cresta lambdoidea; n, ossa nasali; nf, fossa nasale; oc, condilo occipitale; p, parietale; pmx, premascellare; p-sq, sutura tra parietale e squamoso; soc, sopraoccipitale; sop, processo sovraorbitario del frontale;sq-c, apertura interna dello squamoso; tf, fossa temporale; zyg, processo zigomatico dello squamoso.*

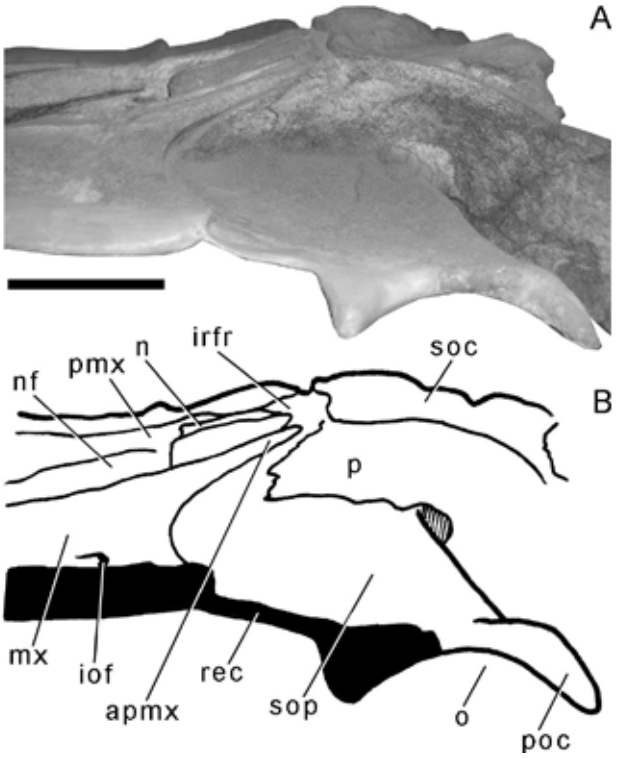

Fig. 5 - *"Megaptera" hubachi*, left dorsolateral view of skull showing the interdigitation of parietal with the posteromedial elements of the rostrum. A, photo; B, interpretation. Scale bar equals 100 mm. Explanation of abbreviations: apmx, ascending process of the maxilla; irfr, interorbital region of the frontal; mx, maxilla; n, nasal; nf, narial fossa; o, orbit; p, parietal; pmx, premaxilla; poc, postorbital corner of frontale; rec, reconstructed portion of maxilla; soc, supraoccipital; sop, supraorbital process of eh frontal; sq, squamosal; sq-p, squamosal-parietal suture.

Fig. 5 - "Megaptera" hubachi*, norma dorsolateral sinistra del cranio per mostrare l'interdigitazione del parietale con gli elementi posteromediali del rostro. A, foto; B, interpretazione. La barra equivale a 100 mm. Legenda: apmx, processo ascendente del mascellare; irfr, regione interorbitaria del frontale; mx, mascellare; n, osso nasale; nf, fossa nasale; o, orbita; p, parietale; pmx, premascellare; poc, angolo postorbitario del frontale; rec, parte ricostruita del mascellare; soc, sovraoccipitale; sop, processo sovraorbitario del frontale.*

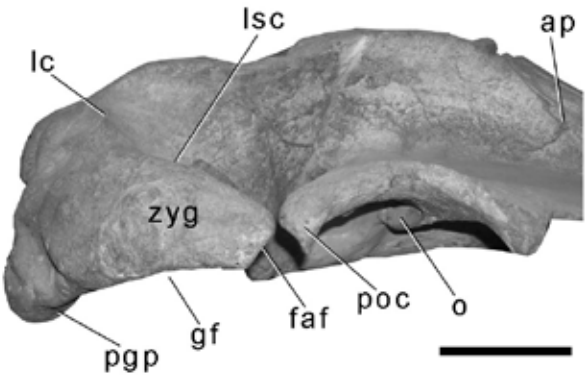

Fig. 6 - *"Megaptera" hubachi*, right squamosal. Scale bar equals 100 mm. Explanation of abbreviations: ap, anterior end of parietal; faf, facet for postorbital corner of supraorbital process of frontal; gf, glenoid fossa; lc, lambdoid crest; lsc, lateral squamosal crest; o, orbit; pgp, postglenoid process; poc, postorbital corner; zyg, zygomatic process.
Fig. 6 - "Megaptera" hubachi*, squamoso destro. La barra equivale a 100 mm. Legenda: ap, limite anteriore del parietale; faf, faccetta di contatto tra processo zigomatico dello squamoso e angolo postorbitario del frontale; gf, fossa glenoidea dello squamoso;lc, cresta lambdoidea; lsc, cresta laterale dello squamoso; o, orbita; pgp, processo postglenoideo dello squamoso; poc, angolo postorbitario del frontale; zyg, processo zigomatico dello squamoso.*

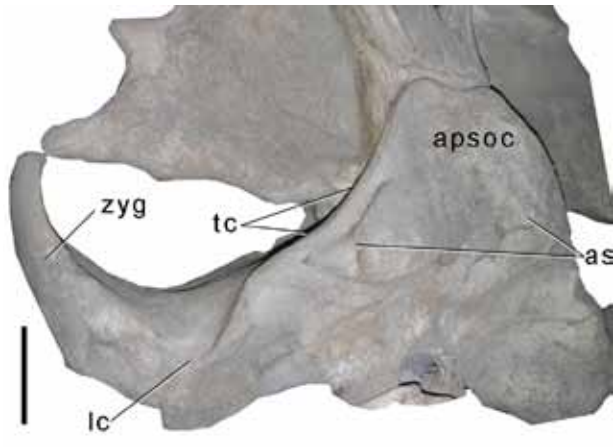

Fig. 8 - Attach sites for neck muscles on the supraoccipital of *"Megaptera" hubachi*. Scale bar equals 100 mm. Explanation of abbreviations: apsoc, anterior portion of supraoccipital; as, attach site for neck muscles; lc, lambdoid crest; tc, temporal crest; zyg, zygomatic process of squamosal.
Fig. 8 - Punti di attacco per la muscolatura del collo sul sovraoccipitale di "Megaptera" hubachi*. La barra equivale a 100 mm. Legenda: apsoc, porzione anteriore del sovraoccipitale; as, siti di attacco per la muscolatura del collo; lc, cresta lambdoidea; tc, creste temporali; zyg, processo zigomatico dello squamoso.*

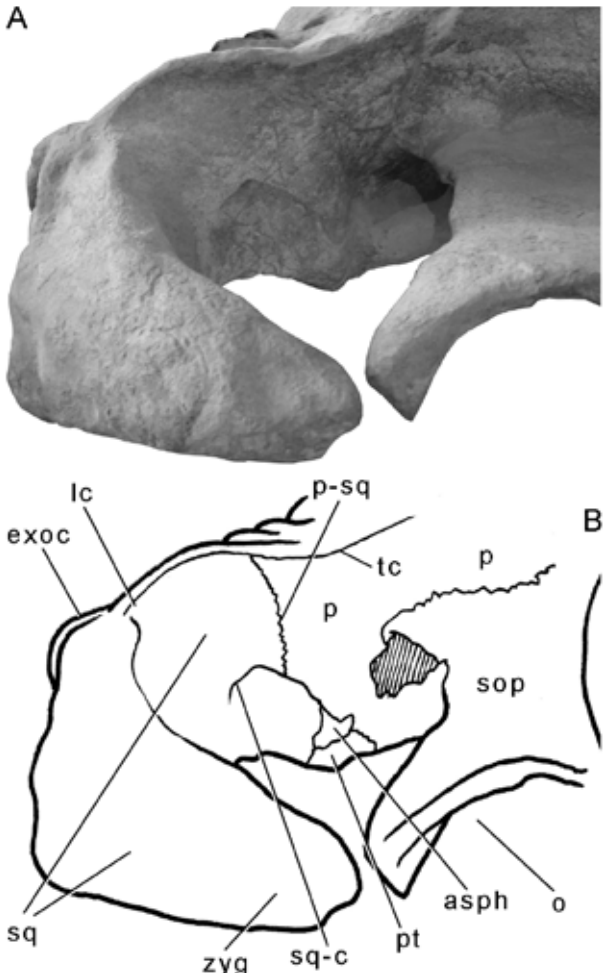

Fig. 7 - The squamosal cleft in the right squamosal of *"Megaptera" hubachi*. A, picture; B, interpretazione. Not to scale. Explanation of abbreviations: asph, alisphenoid; exoc, exoccipital; lc, lambdoid crest; o, orbit; p, parietal; p-sq, squamosal-parietal suture; pt, pterygoid; sop, supraorbital process of squamosal; sq, squamosal; sq-c, squamosal cleft; tc, temporal crest; zyg, zygomatic process of the squamosal.
Fig. 7 - L'apertura interna dello squamoso nello squamoso destro di "Megaptera" hubachi*. A, foto; B, interpretazione. Non in scala. Legenda: asph, alisfenoide;exoc, esoccipitale; lc, cresta lambdoidea; o, orbita; p, parietale; p-sq, sutura tra parietale e squamoso; pt, pteriogoideo; sop, processo sovraorbitario dello squamoso; sq, squamoso; sq-c, apertura interna dello squamoso; tc, cresta temporale; zyg, processo zigomatico dello squamoso.*

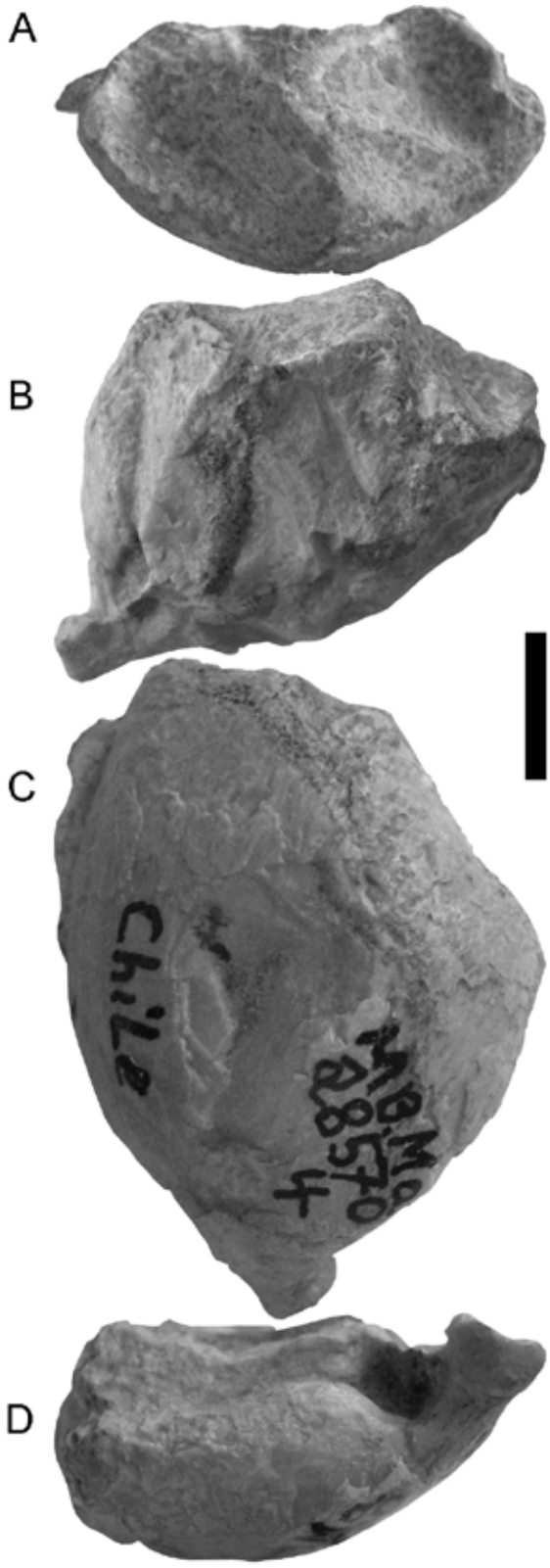

Fig. 9 - "*Megaptera" hubachi*, right pars cochlearis in A, medial; B, dorsal; C, ventral; D, posterior views; Scale bar equals 10 mm.
Fig. 9 - "Megaptera" hubachi, *pars cochlearis destra in norma A, mediale; B, dorsale; C, ventrale; D, posteriore. La scala equivale a 10 mm.*

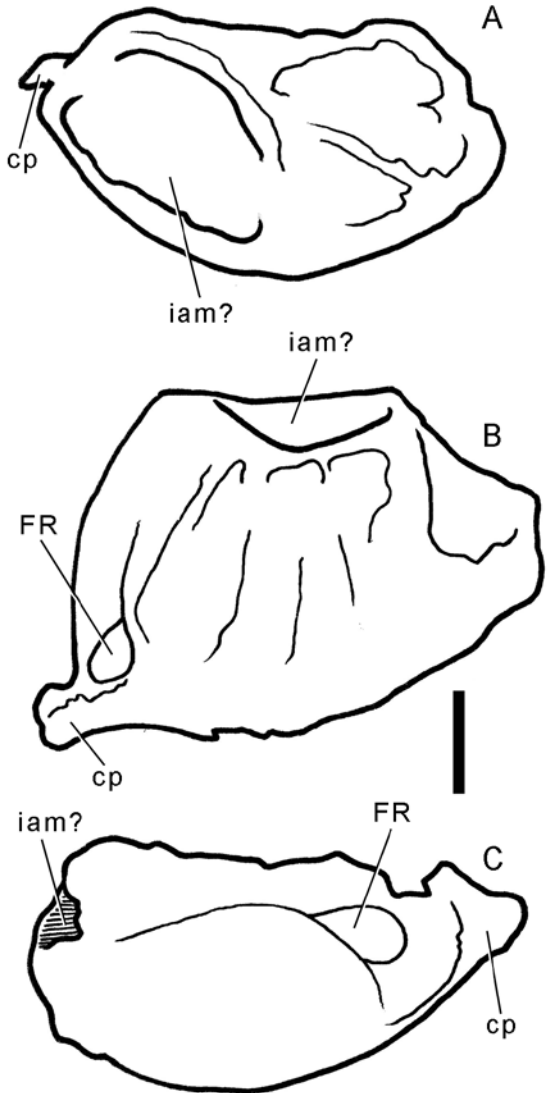

Fig. 10 - Schematic representation of the right pars cochlearis of "*Megaptera" hubachi* in A, medial; B, posterior, C, lateral views. Scale bar equals 10 mm. Explanation of abbreviations: cp, caudal process; FR, round window; iam, internal acoustic meatus.
Fig. 10 - Rappresentazione schematica della pars cochlearis destra di "Megaptera" hubachi *in norma A, mediale; B, posteriore e C, laterale. La barra equivale a 10 mm. Legenda: cp, processo caudale; FR, finestra rotonda; iam, meato acustico interno.*

Dentary

The anterior 75% of both dentaries is not preserved (Figs. 2, 12). The mandibular condyle protrudes dorsally and has a flat posterior articular surface. The angular process is well developed, it is approximately squared and is separated from the condyle by a pterygoid groove which is located laterally and posteriorly. Anteriorly to the condyle, the dorsal border of the ramus is straight. The coronoid process is triangular and has a rounded dorsal border with an apical

Fig. 11 - Anterior process of the periotic of "*Megaptera*" *hubachi* in dorsal view. Scale bar equals 10 mm. Explanation of abbreviations: a, anterior; p, posterior.
Fig. 11- Processo anteriore del periotico di "Megaptera" hubachi *in norma dorsale. La barra equivale a 10 mm. Legenda: a, anteriore; p, posteriore.*

tubercle. The posterior border of the coronoid process descends posteriorly and forms a long postcoronoid crest with a wide postcoronoid fossa.

Anteriorly to the coronoid process, the ventral border of the dentary is sharply-edged. The mandibular foramen is wide and lacks the anterior fissure present in modern balaenopterids. Mental and gingival foramina are not preserved.

Measurements are provided in Table 1.

Vertebrae

The skeleton shows the following vertebral sequence: 7 cervical vertebrae (hereinafter, C1-C7), 11 thoracic vertebrae (T1-T11), 9 lumbar vertebrae (L1-L9), 1 sacral vertebrae (S1), and possibly 19

Distance between mandibular condyle and angular process	120
Height of coronoid process	174
Distance between condyle and coronoid process	302
Distance between coronoid process and apex of dentary	1240
Linear length of dentary	1570
Length of dentary along the curved, external line	1580

Tab. 1 - Measurements of the rigth dentary of " *Megaptera*" *hubachi*. Data in mm.
Tab. 1- Misure della mandibola destra di "Megaptera" hubachi. *Dati in mm.*

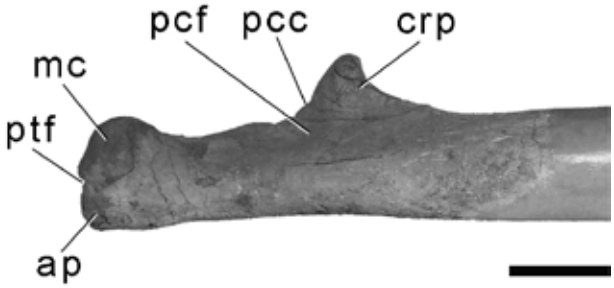

Fig. 12 - Posterior portion of the right dentary of "*Megaptera*" *hubachi*. Scale bar equals 100 mm. Explanation of abbreviations: ap, angular process; crp, coronoid process; mc, mandibular condyle; pcc, postcoronoid crest; pcf, postcoronoid fossa; ptf, pterygoid fovea.
Fig. 12 - Porzione posteriore del ramo mandibolare destro di "Megaptera" hubachi. *La barra equivale a 100 mm. Legenda: ap, processo angolare; crp, processo coronoideo; mc, condilo mandibolare; pcc, cresta postcoronoidea; pcf, fossa postcoronoidea; pcf, fovea pterigoidea.*

caudal vertebrae (Cd1-Cd19). However, at least 11 caudal vertebrae were lacking from the skeleton and were reconstructed in laboratory (Fig. 3).

The seven cervical vertebrae are well preserved. The atlas has a low and triangular neural process; the transverse process is short and squared and its dorsomedial process is located at the emergence of the neural arc. The articular facet for the occipital condyle is highly concave but the articular surface for the axis is flat.

The axis shows a high neural arc with prezygapophyses and wide foramen transversarium which is totally bounded by the dorsal and ventral transverse processes. These fuses at their distal ends. In no other cervical vertebra the foramen transversarium is included between the transverse processes.

The 3rd, 4th, 5th and 6th vertebrae have dorsal and ventral transverse processes; in the 7th the ventral transverse process is lacking.

In the thoracic vertebrae, the emergence of the transverse process is located more dorsally in the more anterior ones and more ventrally in the more posterior ones. The prezygapophyses are flat and transversely wide in the more anterior vertebrae but they become located in the higher part of the neural arc and acquire a triangular shape in the more posterior ones. The series that includes T1-T6 shows prezygapophyses located on the transverse process; in T7-T11 the prezygapophyses are located on the neural arc. In T1-T9 the lateral border of the transverse pro-

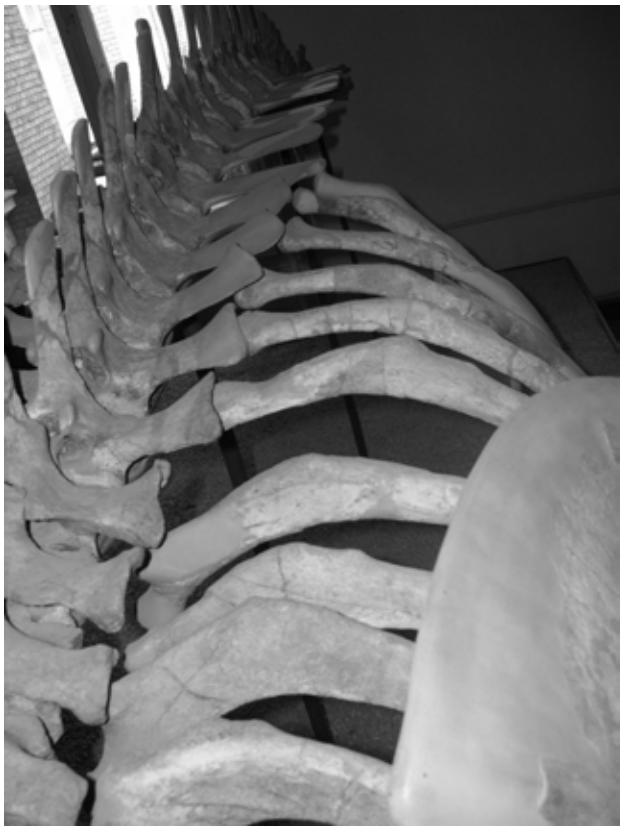

Fig. 13 - Dorsolateral view of the thoracic vertebrae of "*Megaptera" hubachi*. Not to scale.
Fig. 13 - Visione dorsolaterale delle vertebre toraciche di "Megaptera" hubachi. *Non in scala.*

cess is ventrally concave to articulate with the rib articular heads; in these vertebrae, the emergence of the transverse process is located ventrally to the neural arc. In the last two thoracic vertebrae the emergence of the transverse process is located in the higher part of the lateral wall of the vertebral body.

In the lumbar vertebrae, the laterodorsal and lateroventral surfaces of the vertebral body is highly concave both dorsoventrally and anteroposteriorly; the ventral surface displays a sharp keel. The transverse process is located invariably at the middle of the height of the vertebral body.

The sacral vertebra shows a widening and flattening of the ventral surface posteriorly to the ventral keel.

Only 3 caudal vertebrae are preserved. These show well developed emergence of the transverse process and highly concave ventral surface due to the presence of the attach sites for the chevron. Only one intact and one fragmentary chevrons are preserved.

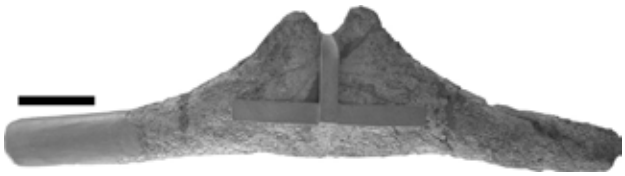

Fig. 14 - "*Megaptera" hubachi*, hyoid in ventral view. Scale bar equals 100 mm.
Fig. 14 - "Megaptera" hubachi*, ioide in norma ventrale. La barra equivale a 100 mm.*

Ribs

Eleven pairs of ribs are present in the skeleton (Figs 3, 13). The first rib is flat and its distal-most portion is concave and thick; its distal border is squared. The five anterior-most ribs have bifid articular head. The ileocostal tuberosity is slightly developed in most of the ribs; it is well developed only in the 5th and 6th of the left side, and on the 3rd rib of the right side.

Sternum

The xiphoid process is subtle, elongated and terminates with a pointed end. The lateral wings are wide and show pointed ends located posterolaterally. The anterior and lateral borders are concave.

Hyoid

Thyrohyoids and basihyoid are fused together to form a short but wide hyoid apparatus. The anterior border of the basihyoid shows two relieves that are directed anteriorly and form the articular surfaces for the descending process of the basioccipital. The thyrohyoids are very elongated and subtle and project posteriorly and laterally (Fig. 14). The stylohyoids are absent.

Forelimb

The forelimb of *"Megaptera" hubachi* shows many characters that can be found in living balaenopterids. Among them, the most striking ones are that the ulna and radius are much longer than the humerus and the presence of 4 digits in the hand (Fig. 15).

The scapula is elongated anteroposteriorly and rather high dorsoventrally (Fig. 15). The posterior border is directed posterodorsally and meets the dorsal border through a nearly right angle. The anterior border is much more dorsally oriented. The acromion is large and is located rather dorsally with respect to the glenoid fossa. The supraspinous fossa is anteroposteriorly short

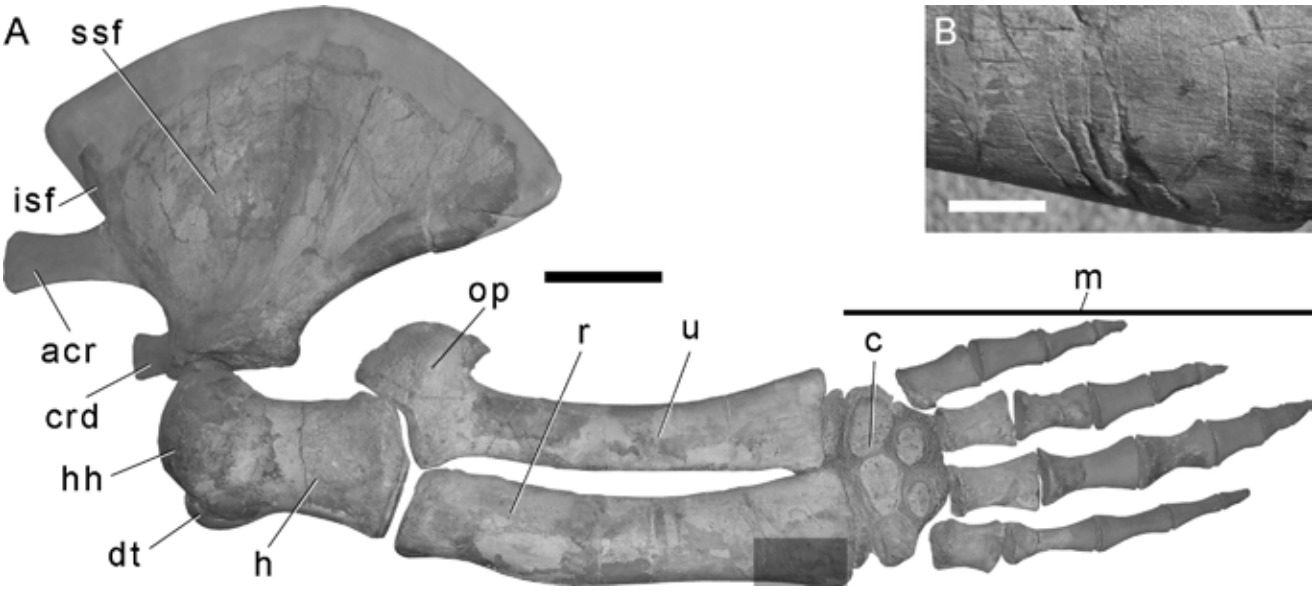

Fig. 15 - "*Megaptera" hubachi*, left forelimb. A, forelimb; B, detail of shark bite marks in the part evidenced by the dark rectangle in the distal epiphysis of radius in A. Scale bars equal 100 mm in A and 10 mm in B. Explanation of abbreviations: acr, acromion process; c, carpals; crd, coracoid process; dt, dorsal trocanther; h, humerus; hh, head of humerus; isf, infraspinous fossa; m, manus; op, olecranon process of ulna; r, radius; ssf, supraspinous fossa; u, ulna.
Fig. 15 - "Megaptera" hubachi, arto anteriore sinistro. A, arto; B, dettaglio dei segni lasciati da uno squalo nella parte evidenziata dal rettangolo scuro nell'epifisi distale del radio mostrato in A. Le barre equivale a 100 mm in A e a 10 mm in B. Legenda: acr, processo acromiale della scapola; c, ossa carpali; crd, processo coracoideo della scapola; dt, trocantere dorsale; h, omero; hh, testa dell'omero; isf, fossa infraspinosa; m, manus; op, processo olecranico dell'ulna; r, radio; ssf, fossa supraspinosa; u, ulna.

and can be observed only dorsally to the scapular spine. The infraspinous fossa is widely concave. The glenoid fossa is only slightly concave. The coracoid process projects anteriorly and medially from the anterior border of the glenoid fossa.

The humerus shows a large and rounded articular head that is separated from the dorsomedial tubercle by a narrow incisure (Fig. 15). The dorsomedial tubercle is well developed and projects anteriorly. The anterior and posterior borders of the diaphysis are broadly straight and parallel. The articular facet for the radius is well separated from that for the ulna by a low relief. The articular facet for the olecranon process of the ulna is small and relatively undeveloped.

The length of the radius is at least three times the length of the humerus (Fig. 15). The radius is elongated with a straight posterior border and a slightly convex anterior border. The distal portion is widened anteroposteriorly. Slightly ventrally to the proximal epiphysis there is a shallow concavity in the anterior border of the radius; shark bite marks are evident near the distal portion of the left radius. The distal epiphysis is not fused with the diaphysis; it is rather rounded and its anteroposterior diameter is lower than that of the distal portion of the diaphysis. The distal part of the radius shows shark bite marks (Fig. 15)

The ulna is highly elongated (Fig 15). The anterior and posterior borders of the diaphysis diverge distally; the anterior border is rather concave ventrally to the proximal epiphysis. The olecranon process has a rounded posterior border; it is linked to the proximal epiphysis by a straight anterior border and to the posterior border of the ulna by a concave posteroventral border. The distal epiphysis (for the articulation with the carpals) is not fused with the diaphysis and is rather convex in lateral view.

The manus includes four partially preserved digits and the complete series of carpal bones (Figs. 15, 16). The proximal carpals are in articular connection with the distal epiphyses of radius and ulna (Fig. 16). The distal carpals are articulated with the proximal carpals and with the metacarpals. In particular, the trapezoid is articulated with the scaphoid and the lunate, and the unciform is articulated with the lunate and the cuneiform. The proposed digit identities follow Cooper *et al.* (2007a, b).

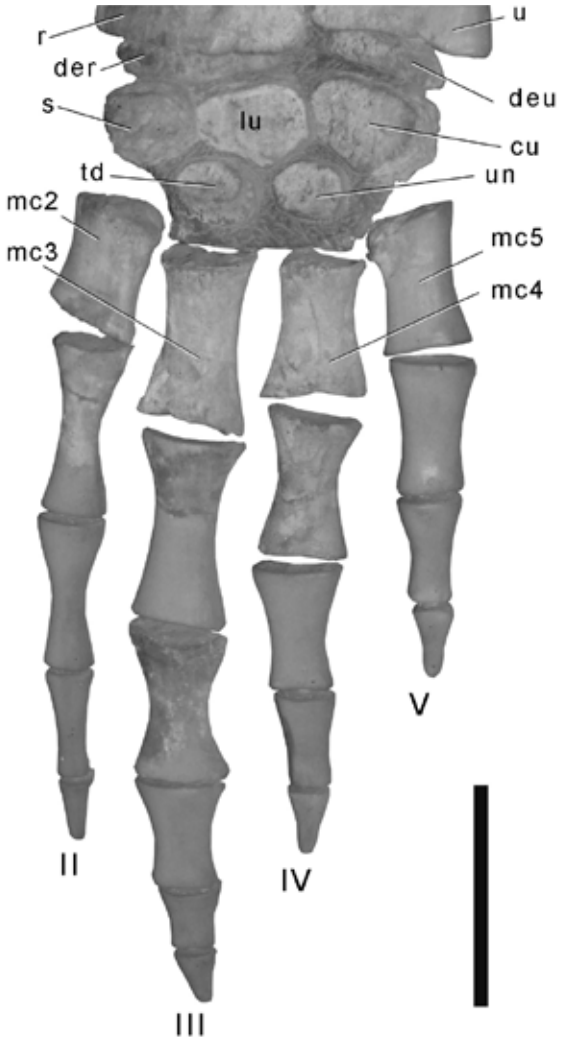

Fig. 16 - The right manus of *"Megaptera" hubachi*. Scale bar equals 50 mm. Explanation of abbreviations: II-IV, 2nd-to-4th digit; cu, cuneiform; der, distal epyphysis of radius; deu, distal epyphysis of ulna; lu, lunate; mc2-5, metacarpals 2-to-5; r, radius; s, scaphoid; td, trapezoid; u, ulna; un, unciform.
Fig. 16 - La manus destra di "Megaptera" hubachi. *La barra equivale a 50 mm. Legenda: II-IV, 2°-4° dito; cu, cuneiforme; der, epifisi distale del radio; deu, epifisi distale dell'ulna; lu, lunato; mc2-5, metacarpali 2-5; r, radio; s, scafoide; td, trapezoide; u, ulna; un, uniforme.*

Analysis of feeding-related traits

In previous analyses of the morphological correlates of feeding in living and fossil mysticetes, the character usually discussed include: (1) the supraorbital process of the frontal (Lambertsen *et al*., 1995), (2) the glenoid fossa of the squamosal (Sanderson, Wassersug, 1993), (3) the condyle and the coronoid process of the dentary (Bisconti, 2007a, b, 2010; Bisconti, Varola, 2006; Kimura, 2002). In the following text these characters are discussed as far as the morphology exhibited by *"Megaptera" hubachi* is concerned.

Morphology

Supraorbital process of the frontal. In *"Megaptera" hubachi* the supraorbital process of the frontal is both abruptly depressed from the interorbital region of the frontal and highly widened anteroposteriorly resembling a sort of wing. The temporal ascending crest is not visible on the dorsal surface of the supraorbital process as observed in living balaenopterids. Both characters strongly suggest that the anterior portion of the temporalis muscle attached the frontal in the same manner as observed in living balaenopterids. It is very likely that the frontomandibular stay described in living balaenopterids by Lambertsen *et al.* (1995) was in place in *"Megaptera" hubachi* given that the living species and this fossil share the same osteological morphology.

Glenoid fossa of the squamosal. In the living species of *Balaenoptera* the glenoid fossa of the squamosal forms a sort of crescent with highly concave articular surface for the occipital condyle of the dentary. In such species, the zygomatic process of the squamosal projects anteriorly and ventrally reaching a point which is approximately at the same height as the postglenoid process. In *Megaptera novaeangliae* the postglenoid process projects sharply ventrally and the zygomatic process of the squamosal projects markedly laterally but not ventrally. In this way, in the living humpback whale the glenoid fossa of the squamosal is highly concave but it is faced mainly anteriorly. In the Piacenzian balaenopterid *Archaebalaenoptera castriarquati* both the postglenoid and the zygomatic processes do not project ventrally at all and the glenoid fossa of the squamosal is straight.

In *"Megaptera" hubachi* the glenoid fossa of the squamosal is rather different from that of the living balaenopterids. In fact, in this taxon, the glenoid fossa is not highly concave but it is straight. This suggests that the ranges of movements that the dentary was able to perform was somewhat different from that of living balaenopterids.

The shape of the glenoid fossa has been put into relation with the presence of the elastic tissue that is located at the craniomandibular joint (Sanderson, Wassersug, 1993; Pivorunas, 1979). This tissue has a fundamental role in preserving mechanical energy during the opening of the

mouth (Sanderson, Wassersug, 1993; Lambertsen, 1983; Pivorunas, 1979). The straight glenoid fossa of the squamosal suggests that in *Archaebalaenoptera castriarquati* such tissue was absent (Bisconti, 2007a); given that also in *"M." hubachi* the glenoid fossa is substantially straight, it must be concluded that the tissue was absent also in this species.

Dentary. The posterior portion of the dentary of "*Megaptera*" *hubachi* is sufficiently well preserved to be analysed in the context of the evolution of feeding behaviour in balaenopterid whales. The mandibular condyle is posteriorly flat as in living balaenopterids and it is sharply bounded by a ventral pterygoid fovea which separates it from the angular process. The latter is rather broad and serves as a wide attach site for the masseter muscle and, medially, for the pterygoid muscle. These muscles are used for active opening and closure of the mouth. The closure of the mouth was actively assisted probably by the temporalis muscle which attached onto the apex of the coronoid process and on the wide and deep postcoronoid fossa. The external curvature of the dentary of "*Megaptera*" *hubachi* is difficult to reconstruct as most of the anterior portion of the ramus is missing.

The presence of a sharply-edged ventral border of the dentary suggests that a conspicuous number of ventral throat grooves were present (according to Bisconti, 2010a and literature therein). This is in contrast to what observed in other early balaenopterids such as *Plesiobalaenoptera quarantellii* and *"Plesiocetus" cortesii* var. *portisi* that are supposed to lack ventral throat grooves or to have had only a very low number of them (Bisconti, 2010a).

Tentative reconstruction of feeding behavior

Several characters of *"Megaptera" hubachi* show its commitment to an intermittent ram feeding (*sensu* Sanderson, Wassersug, 1993) similar to that performed by the living Balaenopteridae. In particular, the shape of the supraorbital process of the squamosal and the shape of the lambdoid crest suggest that the temporalis muscle was developed as in living balaenopterids with the possible presence of the frontomandibular stay as described by Lambertsen *et al.* (1995).

The very slight concavity observed in the glenoid fossa of the squamosal is negatively correlated with the presence of the elastic tissue at the craniomandibular joint. This, in its turn, suggests that the mechanism to save and release the mechanical energy loaded during the opening of the mouth was not in place. The shape of the mandibular condyle suggests that the kinds of movements of the dentary were not the same as those performed by living balaenopterids.

Moreover, the presence of postcoronoid crest and fossa and the broad angular process of the dentary suggest that the masticatory muscles were more active than in living balaenopterids during feeding. These anatomical formations have been observed in some fossil balaenopterid whales (*i.e.*, *Plesiobalaenoptera quarantellii*, *Protororqualus cuvieri*) and should be considered plesiomorphic states for Balaenopteridae as they have been described in archaic 'cetothere' mysticetes (*i.e.*, *Parietobalaena palmeri*, *Diorocetus hiatus*, *Pelocetus calvertensis*, *Titanocetus sammarinensis* and so on). The supposed presence of ventral throat grooves suggests that *"Megaptera" hubachi* was able to catch large numbers of prey items as living balaenopterids do. In conclusion, here, it is suggested that *"M." hubachi* performed a muscular-assisted intermittent ram feeding which used also numerous ventral throat grooves.

Further discussion on the implication of feeding-related traits observed in early balaenopterids in the context of rorqual and humpback phylogeny is presented below (see Discussion paragraph).

Phylogenetic relationships

The phylogenetic relationships of *"Megaptera hubachi"* were investigated through a cladistic analysis based on a comprehensive study of mysticete osteology. Character states were individuated and coded based on the author's study of specimens (Bisconti, 2009) and on data published by a number of students (Deméré *et al.*, 2005, 2008; Kimura, Ozawa, 2002; Kimura, Hasegawa, 2010; Geisler, Luo, 1996, 1998; Sanders, Barnes, 2002a, b; Geisler, Sanders, 2005; Bouetel, De Muizon, 2005; Bisconti, 2005, 2007a, b, 2008; Uhen *et al.*, 2007).

The list of the character states used in the cladistic analysis is presented in Appendix 1. The detailed description of balaenopterid species

indicated here with their inventory numbers is provided elsewhere. These species include two new balaenopterids from Peru and one new species from Italy. The matrix used in the cladistic analysis is presented in Appendix 2.

Goal of this study is to understand the phylogenetic relationships of *"Megaptera" hubachi* through a detailed cladistic analysis of mysticetes. Other results obtained from the present analysis will be discussed elsewhere.

Materials and methods

The comparative study of *"Megaptera" hubachi* has been carried out through a comprehensive osteological analysis based upon the specimens listed in Bisconti (2009). In that table, the species, inventory numbers, repository, age, and relevant literature are provided. The high number of specimens examined warrants for a wide coverage of mysticete morphological variation.

The cladistic analysis was performed by using PAUP 4.010b (Swofford, 2002). The tree-bisection-reconnection (TBR) algorithm with one tree held at each step during stepwise addition was employed to find the most parsimonious cladograms. The TBR algorithm was applied to a matrix of 244 osteological and 2 baleen characters scored for 46 taxa. The character list is presented in Appendix 1. Character states were treated as unordered and unweighted under the ACCTRAN character state optimization criterion. The matrix is presented in Appendix 2.

The outgroup taxa included *Protocetus atavus* Fraas, 1904, *Georgiacetus vogtlensis* Hulbert *et al.*, 1996, *Dorudon atrox* (Andrews, 1906), and *Zygorhyza kochii* (Reichenbach in Carus, 1847). The ingroup taxa included representative species of all the known mysticete radiations.

Morphological support at nodes was analyzed by the search for the 50%-majority rule bootstrap tree and by the reconstruction of the distribution of apomorphies at nodes through the dedicate commands of PAUP.

The distance of the most parsimonious solutions from chance was assessed by a randomization test. This consisted in the evaluation of the amount of difference between the length (in steps) of the most parsimonious solutions from a subset of 10000 trees generated equiprobably from the set of all the cladograms that can be generated from the matrix in Appendix 2.

The degree of agreement between the branching order of the most parsimonious solution and the stratigraphic occurrence of the taxa was assessed by the calculus of the Stratigraphic Consistency Index (SCI) of Huelsenbeck (1994) (see Bisconti 2007a, b, 2008 for a discussion on this index). The stratigraphic ages of the taxa used for the calculus of the SCI were obtained from the Paleobiology Database available at http://paleodb.org/cgi-bin/bridge.pl that was mainly compiled by Mark Uhen.

Results

The TBR search resulted in 36 equally parsimonious trees whose strict consensus is presented in Fig. 17. The randomization test revealed that the tree length is significantly ($p < 0.0001$) lower than the lengths of 10000 trees generated equiprobably from the same matrix; in fact, the mean length of the equiprobable trees is 2098.5 steps while that of the most parsimonious trees is 946 steps.

The Consistency Index of the cladogram in Fig. 17 is rather low (CI = 0.3721) and the Retention Index and the Homoplasy Index are high (respectively, RI = 0.7107 and HI = 0.629) suggesting that a large amount of homoplasy is nested in the dataset.

As far as balaenopterids are concerned, the strict consensus tree shows that Eschrichtiidae is the sister group of Balaenopteridae thus confirming the concept of Balaenopteroidea *sensu* Deméré *et al.* (2005). Balaenopteridae includes five clades: (1) Megapterinae (including only *Megaptera novaeangliae*) and Balenopterinae (including only the living species of *Balaenoptera*), (2) a clade including *Archaebalaenoptera castriarquati* and two still undescribed Peruvian balaenopterids, (3) a clade formed by *Protororqualus cuvieri*, *"Plesiocetus" cortesii* var. *portisi*, and an undescribed Italian balaenopterid from Asti (Piedmont), (4) Parabalaenopterinae (including both *Parabalaenoptera baulinensis* and *Plesiobalaenoptera quarantellii*), and (5) a monophyletic group formed by *Diunatans luctoretemergo* and *"Balaenoptera" siberi*. The present results lead to the conclusion that *"Balaenoptera" siberi* does not belong to *Balaenoptera* and needs a different generic name.

The Late Miocene Parabalaenopterinae are the most primitive balaenopterid whales and are the

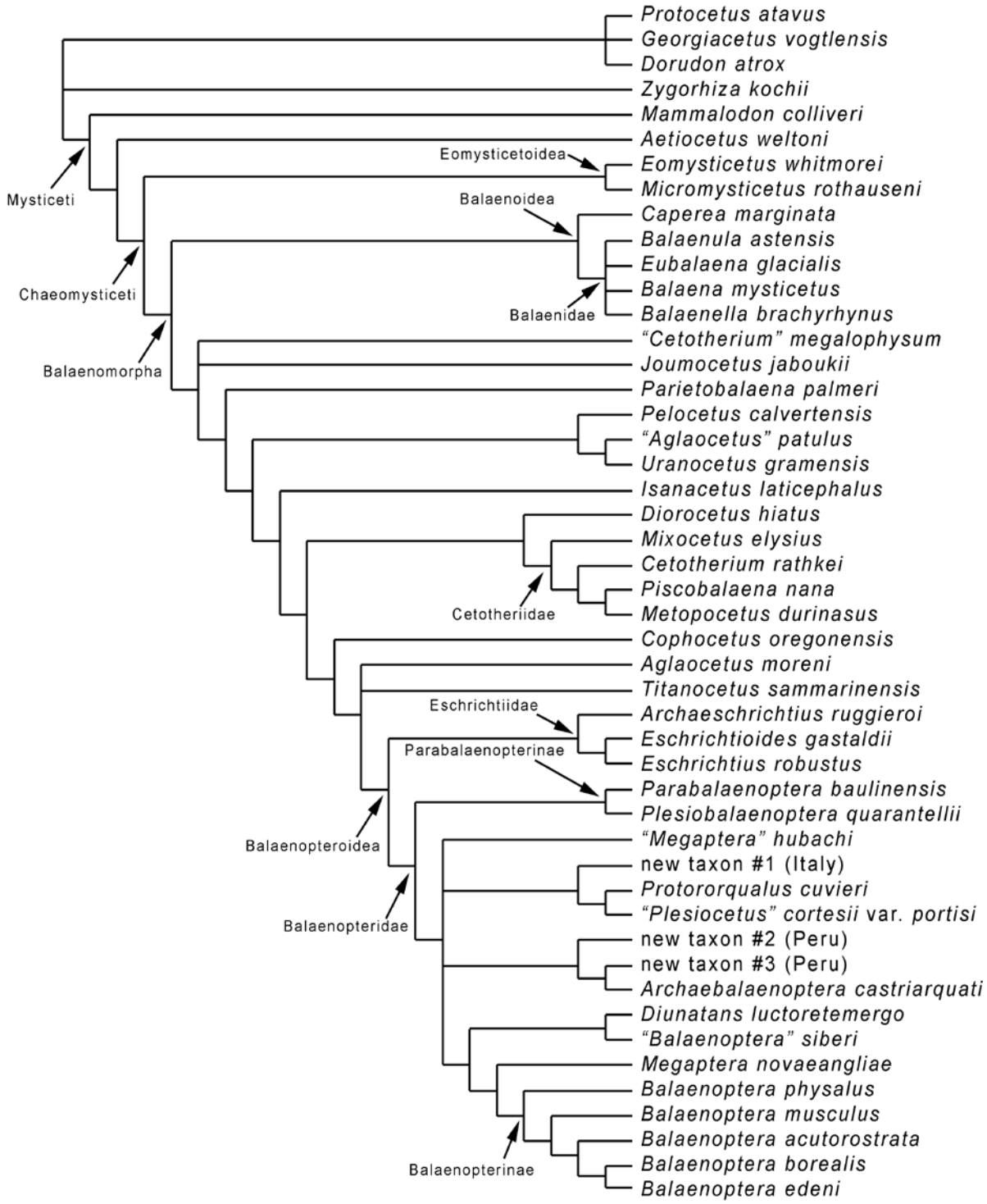

Fig. 17 - Phylogenetic relationships of *"Megaptera" hubachi* as determined by the TBR search. Strict consensus of 36 equally parsimonious trees. Tree statistics: Tree length (TL) = 946 steps; Consistency Index (CI) = 0.3721; Retention Index (RI) = 0.7107; Homoplasy Index (HI) = 0.6279.

Fig. 17 - Relazioni filogenetiche di "Megaptera" hubachi *determinate tramite l'algoritmo TBR. Stretto consenso di 36 cladogrammi egualmente parsimoniosi. Statistiche: Tree length (TL) = 946 steps; Consistency Index (CI) = 0.3721; Retention Index (RI) = 0.7107; Homoplasy Index (HI) = 0.6279.*

sister group of all the other balaenopterids. The clade formed by *Diunatans* and "*B.*" *siberi* is the sister group of Megapterinae + Balaenopterinae. The other two clades (points 2 and 3 above) and "*Megaptera*" *hubachi* form an unresolved polytomy. "*Megaptera*" *hubachi* does not belong to any of the clades described above. From the present result "*Megaptera*" *hubachi* is not monophyletic with *Megaptera novaeangliae* and should receive a different generic name.

The large clade included into the unresolved polytomy of Balaenopteridae is diagnosed by at least 4 characters: character 38(2→3) (position of anterior border of nasal bones at the level of anterior border of supraorbital process of the frontal), character 72(0→1) (lambdoid crest triangular in dorsal view), 92(1→3) (zygomatic process of the squamosal highly divergent from the longitudinal axis of the skull), and 95(2→1) (glenoid fossa of the squamosal shaped as a sort of crescent). Being these the conditions at the branching of clades (1), (2), (3), and (5), it is clear that several reversals occurred in the subsequent radiations. These include the loss of the crescent-shaped glenoid fossa in *Archaebalaenoptera castriarquati* and the zygomatic process of the squamosal which turned to be parallel to the longitudinal axis of the skull in the living species of *Balaenoptera*. Such reversals are not surprising given the high amount of homoplasy indicated by the high values of RI and HI.

The SCI of the TBR resulting tree is 0.727 supporting the consideration that the branching order of the taxa is in broad agreement with their stratigraphic occurrence.

The 50%-majority-rule bootstrap tree is presented in Fig. 18 and shows that there is only limited support for most of the clades individuated in the strict consensus TBR tree of Fig. 21. As far as balaenopterid relationships are concerned, higher bootstrap values support the monophyly of Balaenopteroidea *sensu* Deméré *et al.* (2005) including Eschrichtiidae + Balaenopteridae (75%) and the monophyly of Balaenopteridae (90%). The monophyly of *Protororqualus cuvieri* and "*Plesiocetus*" *cortesii* var. *portisi* is supported by a bootstrap value of 73%. All the other clades received lower bootstrap support values. The monophyly of *Megaptera novaeangliae* and living *Balaenoptera* species is supported by a bootstrap value of 59%.

Synapomorphies of Balaenopteridae as determined by PAUP on the bootstrap tree are several but only three were identified as unambiguous and with CI = 1.0; these are: character 47(0→1) (emergence of supraorbital process of the frontal anteroposteriorly elongated), character 185(-→1) (pterygoid fovea of the dentary scarcely inclined), and 241(0→1) (7th rib with bifid head). While there is no doubt that state 1 of character 47 and state 1 of character 185 are present in all the balaenopterids included into the present analysis in which the character is preserved, it is likely that the synapomoprhic condition for all Balaenopteridae of character 241 depends on the lack of information about the postcranial in fossil balaenopterid whales. In future analyses including also the type materials of Van Beneden's (1882) balaenopterids, probably, the character 185(1) will be dismissed from being a synapomorphic condition of Balaenopteridae or will show lower CI because of more primitive conditions exhibited by these fossils (pers. obs., 2010).

PAUP found also other synapomorphies for Balaenopteridae bu their CI was usually very low. Only 3 of them show a CI > 0.5 and deserve attention; these are: character 81(0→1) (squamosal cleft with distinctive ventral projection at the lateral end), character 150(-→1) (triangular anterior process of the periotic with straight-to-convex anterior border), 166(1→2) (keeled ventral surface of tympanic bulla), and 184(0→1) (pterygoid fovea of dentary located posteriorly). These characters show low levels of homoplasy (*e.g.*, the squamosal cleft is straight and the bulla is uniformly rounded in "*Plesiocetus*" *cortesii* var. *portisi*).

The lack of resolution observed in the bootstrap tree is reasonably due to the high amount of homoplasy present in the dataset. To map the character transformations at each node of the TBR cladogram to individuate the homoplastic characters is outside the scopes of the present work but this will be an important task to be performed and published in a dedicated paper.

Discussion

Taxonomy and phylogeny of "Megaptera" hubachi.

Even after the present study, "*Megaptera*" *hubachi* is still a problematic taxon. The comparative

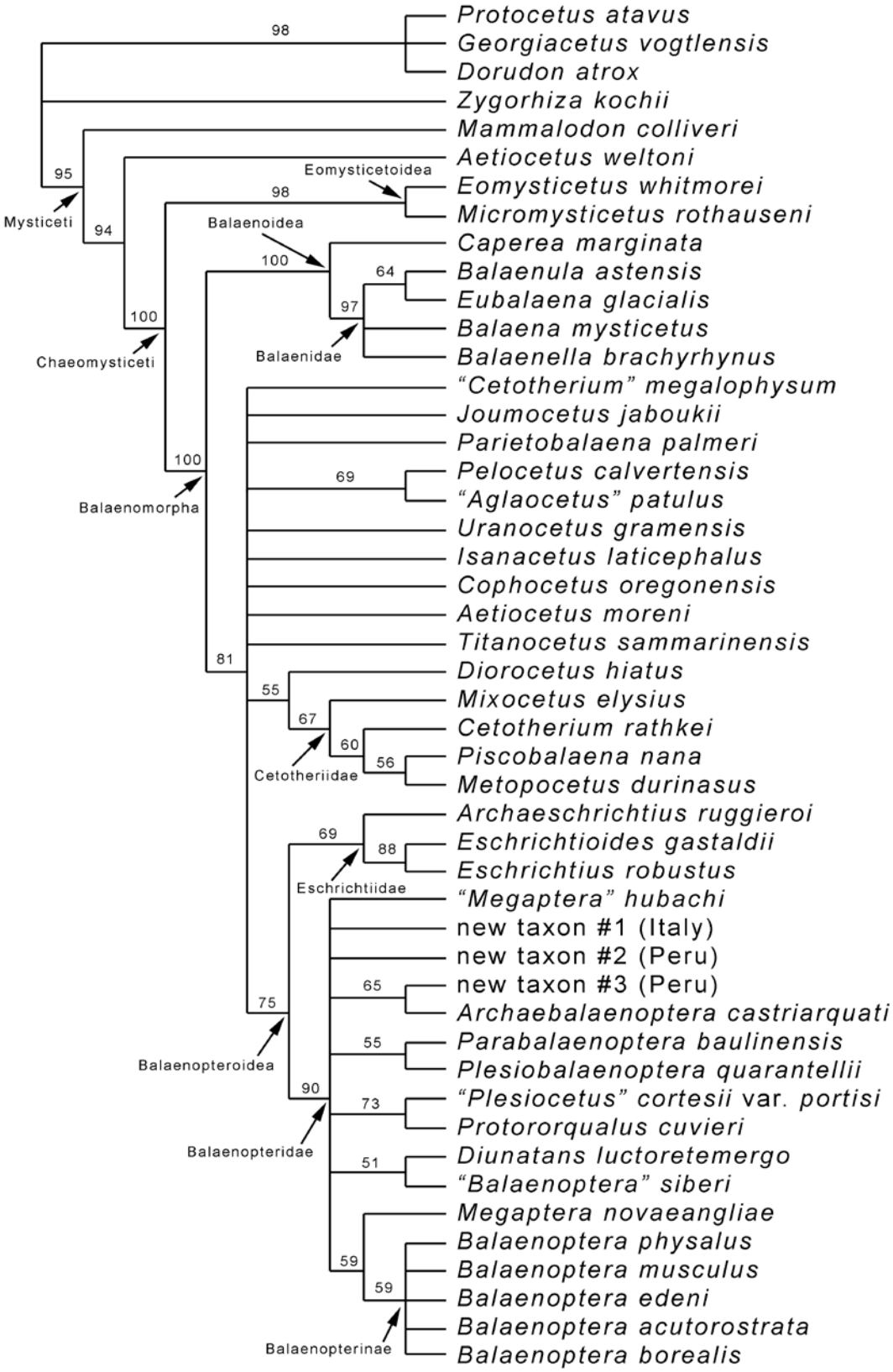

Fig. 18 - Phylogenetic relationships of *"Megaptera" hubachi* as determined by the search of the 50%-majority-rule bootstrap tree. Tree statistics: TL = 1084 steps; CI = 0.3247; RI = 0.6434; HI = 0.6753.

Fig. 18 - Relazioni filogenetiche di "Megaptera" hubachi *determinate tramite bootstrap (50%-majority-rule). Statistiche: TL = 1084 steps; CI = 0.3247; RI = 0.6434; HI = 0.6753.*

analysis revealed that its morphology is distant from that of *Megaptera novaeangliae* in the shape of the squamosal, frontal, dentary and rostrum. In addition, the phylogenetic analysis performed here does not support the inclusion of *M. novaeangliae* and *"M." hubachi* in the same monophyletic clade thus excluding *"M." hubachi* from belonging to the same genus as *M. novaeangliae*.

In their revision of balaenopteroid whales, Deméré *et al.* (2005) showed that *"M." hubachi* did not possess the apomorphic characters of the living humpback whale and suggested that it could represent a distinctive species of *Balaenoptera*. From the present results, it is evident that *Balaenoptera* includes only crown-balaenopterid species thus preventing *"M." hubachi* from being part of it. *"Megaptera" hubachi* is part of a wide balaenopterid radiation developed before or in parallel with the evolution of Megapterinae + Balaenopterinae. This conclusion is supported by the presence of well developed postcoronoid process and fossa, by the lack of crescent-shaped glenoid fossa of the squamosal, by the presence of strong attach sites for neck muscles in the supraoccipital in *"M." hubachi*.

It is likely that the inclusion of other fossil balaenopterid whales (still under study by the present author and several colleagues) into future analyses will help in solving the unresolved nodes observed in Balaenopteridae to also clarify the phylogenetic relationships of *"Megaptera" hubachi*.

Feeding behavior

The feeding-related traits described above suggest that the intermittent ram feeding as performed by living balaenopterids was not fully developed in *"Megaptera" hubachi*. In fact, while the widening of the supraorbital process of the frontal, the morphology of the mandibular condyle, and the location of the pterygoid fovea suggest that most of the characters typical of the intermittent ram feeding were in place in this whale, the archaic shape of the angular process, the straight glenoid fossa of the squamosal, and the presence of the postcoronoid crest and fossa still point to the presence of an active mechanism for the depression and the lifting of the lower jaw in the absence of a mechanism to save energy.

In Fig. 19 four feeding-related morphological characters are mapped onto the phylogeny of Balaenopteridae as determined by the TBR search described above. The characters include: (1) presence of postcoronoid crest and fossa, (2) straight dentary, (3) strongly bowed dentary, and (4) concave glenoid fossa of the squamosal. In Fig. 19, the characters are mapped only in correspondence of the taxa in which they have been found and described. Postcoronoid crest and fossa are present in *Plesiobalaenoptera quarantellii*, *Protororqualus cuvieri*, *"Plesiocetus" cortesii* var. *portisi*, *"Megaptera" hubachi*, and in the living *Balaenoptera* species. In the latter the character is vestigial but present (Bisconti, 2010). The dentary is substantially straight in *Archaebalaenoptera castriarquati*, *Protororqualus cuvierii* and *"Plesiocetus" cortesii* var. *portisi*. On the contrary, the dentary is outwardly bowed in Parabalaenopterinae, *"Balaenoptera" siberi*, *Megaptera novaeangliae* and living *Balaenoptera*. Finally, the glenoid cavity is not concave only in *Archaebalaenoptera castriarquati* and *"Megaptera" hubachi*.

The application of Fitch's (1984) parsimony allows the reconstruction of character states at each node of a cladogram. In Fig. 20 the four feeding-related traits are mapped based upon the application of Fitch's (1984) parsimony. It appears evident that the concave glenoid fossa of the squamosal is a primitive condition for balaenopterids (Fig. 20D) and that the straight dentary was developed only in the *Archaebalaenoptera* + Peruvian 1 and in the *P. cuvieri* + *"P." cortesii* var. *portisi* clades (Fig. 20B). Almost linear dentaries are observed in several archaic 'cetothere' mysticetes such as *Parietobalaena palmeri* and *Diorocetus hiatus* but, despite that, it seems that there is not a phylogenetic structure in the distribution of this character. The presence of postcoronoid crest and fossa is distributed in several taxa but the lack of information from *Archaebalaenoptera* and the undescribed balaenopterids from Peru and Italy prevents the recognition of it as plesiomorphic status of Balaenopteridae (Fig. 20A).

Numerous ventral throat grooves are observed only in *Megaptera novaeangliae* and in the living species of *Balaenoptera*; only *"Megaptera" hubachi* is inferred to possess a high number of ventral throat grooves. Presently, it is impossible to state if it evolved such a character independently from Megapterinae and Balaenopterinae or if all these taxa shared a common ancestor because of the lack of resolution of the cladogram.

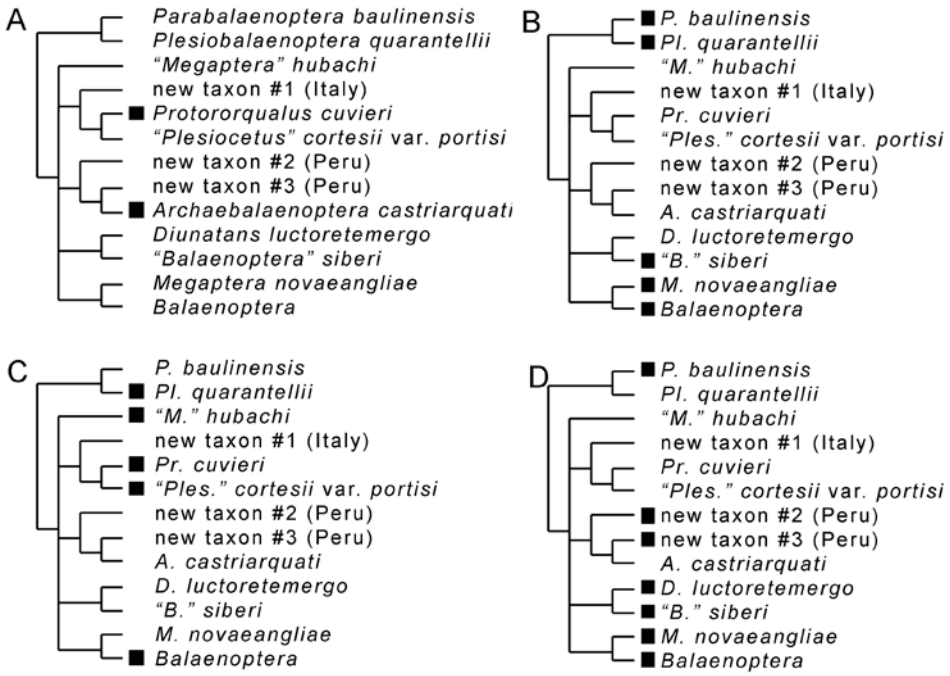

Fig. 19 - Map of presence/absence of four feeding-related traits on the balaenopterid phylogeny (part of Fig. 17). A, straight dentary; B, strongly bowed dentary; C, postcoronoid crest and fossa; D, concave glenoid fossa of the squamosal.
Fig. 19 - Mappa di presenza/assenza di quattro caratteri legati all'alimentazione sulla filogenesi dei balenotteridi (parte di Fig. 17). A, ramo mandibolare lineare; B, ramo mandibolare fortemente incurvato all'esterno; C, cresta e fossa postcoronoidea; D, fossa glenoidea dello squamoso concava.

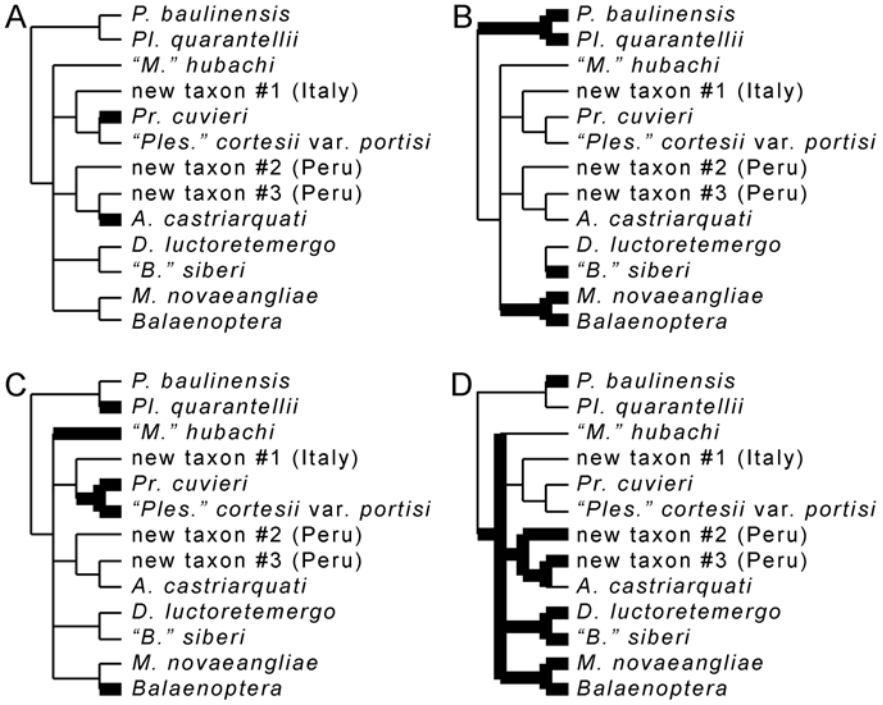

Fig. 20 - Map of presence/absence of four feeding-related traits as in Fig. 19 after the application of Fitch's (1984) parsimony to reconstruct the character states at nodes. A, straight dentary; B, strongly bowed dentary; C, postcoronoid crest and fossa; D, concave glenoid fossa of the squamosal.
Fig. 20 - Mappa di presenza/assenza dei quattro caratteri legati all'alimentazione presentati in Fig. 19 dopo l'applicazione della Fitch's (1984) parsimony per ricostruire gli stati dei caratteri ai nodi. A, ramo mandibolare lineare; B, ramo mandibolare fortemente incurvato all'esterno; C, cresta e fossa postcoronoidea; D, fossa glenoidea dello squamoso concava..

In summary, the concave glenoid fossa of the squamosal is a primitive condition of Balaenopteridae. Given that the morphology of the mandibular condyle is also typical in Balaenopteridae, it appears that this family was early characterized by a peculiar condition at the craniomandibular joint which could be related to an early appearance of the elastic tissue. If this reasoning is accepted, then we must infer that such a tissue was secondarily lost in *Archaebalaenoptera castriarquati* and *"Megaptera" hubachi* where the glenoid fossa of the squamosal is straight. The elastic tissue at the craniomandibular joint should be interpreted as a key-innovation in the evolution of mysticetes; such an innovation triggered the origin and evolution of the highly diversified balaenopterid whales. The subsequent optimization of living *Megaptera novaeangliae* and *Balaenoptera* species would include the strong reduction of muscular assistance to the opening and closing the mouth with the consequent reduction of extension of the postcoronoid crest and fossa and the reduction of the angular process of the dentary.

The determination of the precise sequence of character transformation will be allowed only when the polytomy observed in post-parabalaenopterine balaenopterids will be resolved. That operation will allow the full comprehension of the tempo and mode of evolution of the highly specialized feeding mechanism of the living Balaenopteridae.

Relationships of South American balaenopterid whales.

Four fossil balaenopterid whales were included into the phylogenetic analysis presented here for the first time. Deméré *et al.* (2005) included only *"Balaenoptera" siberi* and *"Megaptera" hubachi* into their study and found that both were part of a clade including also the living fin whale *Balaenoptera physalus*. In a combined molecular and morphological analysis they found that they were part of a clade including also *Megaptera novaeangliae* and *Balaenoptera physalus*. Such a result was also confirmed by another study published by Deméré *et al.* (2008).

From the present analysis, *Megaptera novaeangliae* and *Balaenoptera physalus* belong to a clade that does not include *"Megaptera" hubachi* and *"Balaenoptera" siberi*. The inclusion of two additional balaenopterids from Peru in the present phylogenetic analysis provides completely different results and suggests the existence of different subfamily-rank clades corresponding to different balaenopterid radiations.

South American balaenopterids are included in three distinct radiations: (1) a clade including also *Archaebalaenoptera castriarquati*, (2) a clade formed by *Diunatans luctoretemergo* + *"Balaenoptera" siberi*, and (3) the separate and unresolved position of *"Megaptera" hubachi*. This result shows that balaenopterids experienced widespread distribution during the Neogene with supraspecific taxa occurring in both the austral and boreal hemispheres. This observation allows to infer that balaenopterids crossed the Equator maybe more times in the latest Miocene and Pliocene and gave rise to northern and southern forms.

The inclusion of the balaenopterid specimens currently under study in future phylogenetic analyses will be of great help in resolving the unresolved nodes in the balaenopterid phylogeny. After that, it will be possible to realize a phylogeny-based paleobiogeographic analysis of the family able to reveal how they could attain the distribution pattern that balaenopterid fossils document.

Conclusions

"Megaptera" hubachi does not show the apomorphic features typical of *Megaptera novaeangliae*. Both comparative morphology and phylogenetic analysis exclude that these taxa form a monophyletic clade, thus, they must be assigned to different genera. For this reason, a new generic name must be created for *"Megaptera" hubachi*.

The morphological analysis of feeding-related morphological characters preserved in the skull and dentary of *"Megaptera" hubachi* revealed that most of the features associated to the intermittent ram feeding of living balaenopterids were present. These include the concave glenoid fossa of the squamosal, the wide and depressed supraorbital process of the frontal, the flat and posteriorly-oriented mandibular condyle, the posterior placement of the pterygoid fovea under the mandibular condyle, and the sharply-edged ventral border of the dentary. The last character is probably related to the presence of a high number of ventral throat grooves which are, thus, inferred to be numerous in this taxon. However, the presence of a well developed angular process and of

the postcoronoid crest and fossa suggest that the opening and closure of the mouth were assisted by active muscular actions in contrast to what is observed in the living balaenopterid whales.

The phylogenetic relationships of "*Megaptera*" *hubachi* are still largely unresolved despite the massive morphological and taxonomic samplings realized here. This form belongs to a wide, unresolved radiation including several and still undescribed subfamily-rank taxa whose identification reveals that the balaenopterid phylogeny was much more complex than expected based on previous studies. The analysis revealed also high levels of homoplasy which made it impossible to find high bootstrap support values.

The feeding-related traits evolved in complex patterns in the phylogeny of balaenopterids. It was possible to infer that the concave glenoid fossa of the squamosal is primitive in Balaenopteridae but it was not possible to unambiguously reconstruct the phylogenetic history of the postcoronoid crest and fossa, the degree of outward bowing of the dentary, and the evolution of numerous ventral throat grooves. Other work is needed to unambiguously reconstruct the evolutionary history of balaenopterid feeding mechanisms.

Acknowledgments

I am indebted to to Oliver Hampe (Museum für Naturkunde, Berlin) who provided very kind and useful assistance during my visit in 2009. He also reviewed the manuscript providing insightful suggestions that highly improved it.

References

Bisconti M., 2010a. A new balaenopterid whale from the Miocene of the Stirane River, northern Italy (Mammalia, Cetacea, Mysticeti). J. Vert. Pal., 30: 943-958.

Bisconti M., 2010b. Cenozoic environmental changes and evolution of baleen whales. In: Murray C.A. (ed), Whales and dolphins: behavior, biology and distribution. Nova Publishing, New York, pp. 1-46.

Bisconti M., 2009. Taxonomy and evolution of the Italian Pliocene Mysticeti (Mammalia, Cetacea): a state of the art. Boll. Soc. Pal. It., 48: 147-056.

Bisconti M., 2007a. A new basal balaenopterid whale from the Pliocene of northern Italy. Palaeontology, 50: 1103-1122.

Bisconti M., 2007b. Taxonomic revision and phylogenetic relationships of the rorqual-like mysticete from the Pliocene of Mount Pulgnasco, northern Italy (Mammalia, Cetacea, Mysticeti). Palaeontogr. It., 91: 85-108.

Bisconti M., 2003. Evolutionary history of Balaenidae. Cranium, 20: 9-50.

Bisconti M., Varola A., 2006. The oldest eschrichtiid mysticete and a new morphological diagnosis of Eschrichtiidae (gray whales). Riv. It. Pal. Strat., 112: 447-457.

Bosselaers M., Post K., 2010. A new fossil rorqual (Mammalia, Cetacea, Balaenopteridae) from the Early Pliocene of the North Sea, with a review of the rorqual species described by Owen and Van Beneden. Geodiversitas, 32: 331-363.

Bouetel V., Muizon C., 2006. The anatomy and relationships of *Piscobalaena nanna* (Cetacea, Mysticeti), a Cetotheriidae s.s. from the early Pliocene of Peru. Geodiversitas, 28: 319-395.

Brand L.R., Esperante R., Chadwick A.V., Poma Porras O., Alomía M., 2004. Fossil whale preservation implies high diatom accumulation rate in the Miocene–Pliocene Pisco Formation of Peru. Geology, 32: 165-168.

Caretto P.G., 1970. La balenottera delle sabbie plioceniche di Valmontasca (Vigliano d'Asti). Boll. Soc. Pal. It., 9: 3-75.

Cooper L.N., Dawson S.D., Reidenberg J., Berta A., 2007a. Neuromuscular anatomy and the evolution of the cetacean forelimb. Anat. Rec., 290: 1121-1137.

Cooper L.N., Berta A., Reidenberg J., Dawson S.D., 2007b. Hyperphalangy and digit reduction: evolution of the cetacean manus. Anat. Rec., 290: 654-673.

Dathe F., 1983. *Megaptera hubachi* n. sp., ein fossiler Bartenwal aus marinen Sandsteinschichten des tieferen Pliozäns Chiles. Zeitsch. Geol. Wiss., 11: 813-852.

Deméré T.A., 1986. The fossil whale, *Balaenoptera davidsonii* (Cope 1872), with a review of other Neogene species of *Balaenoptera* (Cetacea: Mysticeti). Mar. Mamm. *Sci.*, 2: 277-298.

Deméré T.A., Berta A., McGowen M.R., 2005. The taxonomic and evolutionary history of fossil

and modern balaenopteroid mysticetes. *J. Mamm. Evol.*, 12: 99-143.

Fitch W.M., 1971. Toward defining the course of evolution: minimal change for a specific tree topology. Syst. Zool., 20:406-416.

Geisler J.H., Luo Z., 1996. The petrosal and inner ear of Herpetocetus sp. (Mammalia: Cetacea) and their implications for the phylogeny and hearing of archaic mysticetes. J. Paleont., 70, 1045-1066.

Geisler J.H., Luo Z., 1998. Relationships of Cetacea to terrestrial ungulates and the evolution of cranial vasculature in Cete. In: Thewissen, J. G. M. (ed), The emergence of whales. Evolutionary patterns in the origin of Cetacea. Plenum Press, New York, pp. 163-212.

Geisler J.H., Sanders A.E., 2003. Morphological evidence for the phylogeny of Cetacea. J. Mamm. Evol., 10, 23-129.

Hampe O., Baszio S., 2010. Relative warps meet cladistics: a contribution to the phylogenetic relationships of baleen whales based on landmark analyses of mysticete crania. Bull. Geosci., 85: 199-218.

Huelsenbeck J.P., 1994. Comparing the stratigraphic record to estimates of phylogeny. Paleobiology, 20, 470-483.

Kimura T., 2002. Feeding strategy of an Early Miocene cetothere from the Toyama and Akeyo Formations, central Japan. Palaeont. Rec., 6: 179-189.

Kimura T., Ozawa T., 2002. A new cetothere (Cetacea: Mysticeti) from the Early Miocene of Japan. J. Vert. Pal., 22: 684-702.

Kimura T., Hasegawa Y., 2010. A new baleen whale (Mysticeti: Cetotheriidae) from the earliest Late Miocene of Japan and a reconsideration of the phylogeny of cetotheres. J. Vert. Pal., 30: 577-591.

Lambertsen R.H., Ulrich N., Straley J., 1995. Frontomandibular stay of Balaenopteridae: a mechanism for momentum recapture during feeding. J. Mamm., 76: 877-899.

Lambertsen R.H., 1983. Internal mechanism of rorqual feeding. J. Mamm., 64: 76-88.

Pilleri G., 1989. *Balaenoptera siberi*, ein neuer Spätmiozäner Bartenwal aus der Pisco-Formation Perus. In: Pilleri G. (ed), Beiträge zur Paläontologie der Cetaceen Perus. Hirnanatomisches Institut Ostermundigen, Bern, pp. 65-107.

Pivorunas A., 1979. The fibrocartilage skeleton and related structures of the ventral pouch of balaenopterid whales. J. Morph., 151: 299-314.

Rychel A.L., Reeder T.W., Berta A., 2004. Phylogeny of mysticete whales based on mitochondrial and nuclear data. Mol. Phyl. Evol., 32: 892-901.

Sanders A.E., Barnes L.G., 2002a. Paleontology of the Late Oligocene Ashley and Chandler Bridge formations of South Carolina: *Micromysticetus rothauseni*, a primitive cetotheriid mysticete (Mammalia: Cetacea). In: Emry R. J. (ed), Cenozoic mammals of land and sea: tributes to the career of Clayton E. Ray. Smithsonian Contributions to Paleobiology, 93: 271-293.

Sanders A.E., Barnes L.G., 2002b. Paleontology of the Late Oligocene Ashley and Chandler Bridge formations of South Carolina 3: Eomysticetidae, a new family of primitive Oligocene mysticetes (Mammalia: Cetacea), from South Carolina, U.S.A. In: Emry R. J. (ed), Cenozoic mammals of land and sea: tributes to the career of Clayton E. Ray. Smithsonian Contributions to Paleobiology, 93: 313-356.

Sanderson L.R., Wassersug R., 1993. Convergent and alternative designs for vertebrate suspension feeding. In: Hanken J., Hall B.K. (eds), The skull. Volume 3: Functional and evolutionary mechanisms. University Press of Chicago, Chicago, pp. 37-112.

Swofford D.L., 2002. PAUP – Phylogenetic Systematics Using Parsimony. Beta Documentation. Laboratory of Molecular Systematics, Smithsonian Institution. Available at http://paup.csit.fsu.edu/

Uhen, M. D., Fordyce, R. E., Barnes, L. G. (2007). Mysticeti. In: Janis C.M., Gunnell G.F., Uhen M.D. (eds), Evolution of Tertiary Mammals of North America. Cambridge University Press, Cambridge, pp. 607-628.

Van Beneden P.-J.,1882. Description des ossements fossiles des environs d'Anvers. Genres: *Megaptera*, *Balaenoptera*, *Burtinopsis*, *Erpetocetus*. Annales du Musee Royal d'Histoire Naturelle de Belgique, 7 (3), 1-90 plus atlas.

Zeigler C.V., Chan G.L., Barnes L.G., 1997. A new Late Miocene balaenopterid whale (Cetacea: Mysticeti), *Parabalaenoptera baulinensis*, (new genus and species) from the Santa Cruz Mudstone, Point Reyes Peninsula, California. *Proc. Cal. Acad. Sci.*, 50: 115-138.

Appendix 1 : Character list for cladistic analysis

Maxilla

1. Rostrum length: 0, rostrum forms around half of the length of the skull; 1, rostrum forms less than half of the skull; 2, rostrum forms more than half of the length of the skull.
2. Rostrum width at base (between bases of lateral processes of the maxillae): 0, rostrum wide; 1, rostrum narrow.
3. Lateral borders of maxilla posteriorly (in dorsal view) (between bases of lateral processes of the maxillae): 0, gently diverging from the longitudinal axis; 1, parallel to longitudinal axis.
4. Lateral borders of maxilla in dorsal view: 0, straight; 1, converging.
5. Rostrum straight in lateral view: 0, yes; 1, no (rostrum anteroposteriorly arched).
6. Rostrum arc: 0, moderate; 1, rostrum highly arched.
7. Rostrum arc: 0, continuous; 1, discontinuous.
8. Lateral process of maxilla: 0, absent; 1, present.
9. Lateral process of maxilla: 0, long; 1, very short to absent; 2, very long.
10. Antorbital groove: 0, absent; 1, present.
11. Antorbital notch: 0, absent; 1, present.
12. Grooves on the palate for vasculature of baleen epithelium: 0, absent; 1, present.
13. Baleen: 0, absent; 1, present.
14. Baleen: 0, long; 1, short.
15. Ascending process of maxilla: 0, absent; 1, present.
16. Ascending process of maxilla: 0, short; 1, long.
17. Ascending process of maxilla: 0, wide at base; 1, narrow at base.
18. Ascending process of maxilla: 0, posteriorly rounded; 1, posteriorly pointed; 2, posteriorly squared.
19. Ascending process of maxilla: 0, located anterior to antorbital corner of frontal; 1, posterior.
20. Ascending process of maxilla: 0, lateral border forms a distinctive angle with posterior border of maxilla; 1, lateral border forms a wide curve with posterior border of maxilla; 2, posterior border forms a straight line inclined towards the longitudinal axis of the skull and posteriorly.
21. Ascending process of maxilla: 0, the distinctive angle is obtuse; 1, the distinctive angle is around 90°.
22. Ascending process of maxilla: 0, terminates at posterior border of nasal; 1, terminates posteriorly to the nasal; 2, terminates anteriorly to the nasal.
23. Ascending processes of maxillae: 0, do not meet posteriorly along midline; 1, meet posteriorly to the nasal along midline.
24. Ascending processes of maxillae: 0, do not meet supraoccipital posteriorly; 1, meet supraoccipital posteriorly.
25. Dorsal exposition of ascending process of the maxilla: 0, wide; 1, narrow because they are exposed laterally on the depression of the supraorbital process of the frontal.
26. Lateral surface of maxilla: 0, vertical; 1, flat and exposed dorsally.
27. Lateral border of maxilla: 0, thick; 1, thin.
28. Posterior border of maxilla: 0, tightly joined with frontal; 1, loosely joined with frontal or no joined at all.
29. Infraorbital foramen: 0, bilateral foramens; 1, distintegrated into a series of foramens.
30. Medial border of maxilla crest-like in the posterior half: 0, no; 1, yes.
31. Infraorbital foramen distribution: 0, scattered in the posterior surface of the maxilla; 1, allineated closely to medial border of maxilla.

Premaxilla

32. Premaxillary foramen: 0, present; 1, absent.
33. Anterior expansion in premaxilla: 0, absent; 1, present.
34. Posterior termination of premaxilla: 0, anterior to posterior end of maxilla; 1, at the same level of maxilla and nasal.
35. Posterior termination of premaxilla if anterior to maxilla: 0, lateral to the nasal; 1, anterior to the nasal.
36. Teeth in maxilla and premaxilla: 0, present; 1, absent.
37. Mesorostral groove: 0, absent; 1, present.

Nasal

38. Anterior end of nasal: 0, close to anterior end of rostrum; 1, around mid-rostrum; 2, slightly anterior to anterior border of supraorbital process of frontal; 3, at the same level of anterior border of supraorbital process of frontal; 4, posterior to anterior border of frontal.
39. Nasal proportions: 0, nasal width much lower than nasal length; 1, nasal width close to nasal length; 2, nasal width higher than nasal length.
40. Width of posterior portion of nasal: 0, rather wide; 1, very thin.
41. Lateral borders of nasal: 0, parallel to longitudinal axis of the skull; 1, anteriorly diverging; 2, anteriorly converging; 3 transversely constricted.
42. Anterior border of nasal: 0, concave; 1, transversely flat; 2, convex; 3, lateral corner more anterior than medial corner.
43. Nasal length relative to condylobasal length: 0, long; 1, moderate; 2, short.
44. Nasal dorsal surface: 0, flat; 1, sagittal keel ante-

rior half.

Lacrimal

45. Lacrimal exposition in dorsal view: 0, lacrimal absent in dorsal view; 1, lacrimal well exposed in dorsal view.

Frontal

46. Supraorbital process of frontal: 0, horizontal and continuous with interorbital region of frontal; 1, gently descending from interorbital region; 2, abruptly depressed from interorbital region.
47. Supraorbital process of frontal: 0, emergence anteroposteriorly narrow; 1, emergence anteroposteriorly elongated.
48. Supraorbital process of frontal: 0, very short; 1, short; 2, long.
49. Posterior border of supraorbital process of frontal: 0, concave; 1, straight.
50. Orientation of anterior border of supraorbital process of frontal: 0, lateral; 1, anterior; 2, posterior.
51. Ascending temporal crest: 0, very evident; 1, evident; 2, reduced to a line.
52. Ascending temporal crest: 0, located on posterodorsal edge of supraorbital process of frontal; 1, developed from postorbital corner of sop to the anteromedial corner of sop; 2, posteriorly concave with lateral end terminating at postorbital corner; 3, located at anterior border of supraorbital process of frontal.
53. Postorbital corner of supraorbital process of frontal shows a clearly visible articular facet for zygomatic process of squamosal: 0, no; 1, yes.
54. Postorbital corner of supraorbital process of frontal far from zygomatic process of squamosal: 0, yes; 1, no, they are close.
55. Coronal (frontoparietal) suture in dorsal view: 0, transversely concave; 1, straight; 2, transversely convex because parietal is superimposed on interorbital region of frontal posteriorly; 3, transversely concave because posteromedial elements of rostrum are interposed between parietal squamae.
56. Posterior contact of interorbital region of frontal in dorsal view: 0, parietal; 1, supraoccipital.
57. Position of nasofrontal suture: 0, within interorbital region of frontal; 1, anterior border of interorbital region of frontal.
58. Anterior exposition of interorbital region of frontal: 0, long; 1, short because posteromedial elements of rostrum are located on it; 2, short because supraoccipital superimposes on it; 3, short because parietal superimposes on it.
59. Paraxial length of interorbital region of frontal: 0, long; 1, very long; 2, short.
60. Interorbital region of frontal forms subtle sheet of bone surrounding ascending process of maxilla: 0, absent; 1, present.
61. Transverse width of interorbital region of the frontal between the depressions of the supraorbital processes of the frontal: 0, narrow; 1, wide.

Jugal

62. Jugal shape: 0, long and mainly straight; 1, short and ventrally rounded.

Parietal

63. Exposition of parietal at vertex: 0, long; 1, short; 2, very short; 3, absent.
64. Sagittal crest formed by parietal at vertex: 0, present; 1, absent.
65. Sagittal crest formed by parietal at vertex: 0, acute; 1, transversely flat and formed by two opposite concavities on both sides of longitudinal axis of the skull.
66. Width between lateral concavities formed by parietal at vertex: 0, short; 1, wide; 2, very wide.
67. Parietal anteriorly overwhelmed by temporal crest: 0, no; 1, yes.
68. Parietal posteriorly overwhelmed by temporal crest: 0, no; 1, yes.
69. Transverse width of postorbital constriction: 0, very narrow; 1, narrow; 2, wide.
70. Elongation of postorbital constriction: 0, very long; 1, long; 2, short.
71. Post-parietal foramen: 0, present; 1, absent.
72. Lambdoid crest in dorsal view: 0, wide and rounded; 1, triangular.
73. Posterior apex of lambdoid crest in dorsal view: 0, anterior or same level of occipital condyles; 1, posterior to occipital condyles.
74. Parietal and squamosal bulging in temporal fossa: 0, absent; 1, present.
75. Strong concavity in temporal fossa posterior to emergence of supraorbital process of frontal: 0, absent; 1, present.
76. Anterior end of parietal: 0, posterior to the posteromedial elements of rostrum; 1, anterior to the posteromedial elements of rostrum (parietal interdigitated with maxilla).
77. Anterolateral portion of parietal squama: 0, superimposed on the emergence of supraorbital process of frontal; 1, not.

Interparietal

78. Interparietal exposition at vertex: 0, absent; 1, present.
79. Anterior border of interparietal: 0, in contact with parietal; 1, in contact with interorbital region of frontal.

Squamosal

80. Squamosal cleft: 0, absent; 1, present.
81. Squamosal cleft shape: 0, straight; 1, lateral part forms a distinctive angle with medial part.
82. Squamosal cleft emergence at adulthood: 0, from squamosal-alisphenoid suture; 1, from parietal-squamosal suture; 2, from squamosal-pterygoid suture.
83. Squamosal cleft emergence during later ontogeny: 0, from parietal-alisphenoid suture; 1, from parietal-squamosal suture; 2, from squamosal-pterygoid suture.
84. Cranio-mandibular joint: 0, close articulation; 1, loose articulation.
85. Cranio-mandibular joint: 0, posterior to orbit and elongated anteroposteriorly; 1, approximately under the orbit and elongated dorsoventrally.
86. Dorsoventral elongation of squamosal: 0, absent; 1, present.
87. Supramastoid crest: 0, absent; 1, present.
88. Secondary squamosal crest: 0, absent; 1, present.
89. Zygomatic process of squamosal in lateral view: 0, long; 1, short; 2, very short.
90. Zygomatic process of squamosal in lateral view: 0, projecting anteriorly; 1, projecting anteriorly and ventrally.
91. Zygomatic process of squamosal in lateral view, lateral fossa: 0 absent; 1, present.
92. Zygomatic process of squamosal in dorsal view (lateral border): 0, projecting medially; 1, projecting anteriorly; 2, projecting anterolaterally; 3, strongly diverging from anteroposterior axis of skull.
93. Apex of zygomatic process of squamosal twisted medially: 0, no; 1, yes.
94. Postglenoid process of squamosal: 0, projecting ventrally much more than zygomatic process; 1, projecting ventrally close to zygomatic process.
95. Glenoid fossa of squamosal in lateral view: 0, right angle; 1, highly concave (crescent-shaped); 2, straight and inclined ventroposteriorly; 3, straight and oriented anteroposteriorly; 4, slightly concave.

Alisphenoid

96. Alisphenoid exposition in temporal fossa: 0, present; 1, absent.
97. Alisphenoid contacts in temporal fossa: 0, alisphenoid between frontal, parietal, squamosal, and pterygoid; 1, alisphenoid between parietal, squamosal, and pterygoid; 2, alisphenoid between parietal and pterygoid; 3, alisphenoid between parietal and squamosal.

Supraoccipital

98. Position of anterior border of supraoccipital: 0, posterior to anterior end of zygomatic process of squamosal; 1, anterior to anterior end of zygomatic process of squamosal.
99. Attach sites for neck muscles on lateral surfaces of supraoccipital: 0, low to absent; 1, present.
100. Attach sites for neck muscles on lateral surfaces of supraoccipital: 0, well developed; 1, strong.
101. Nuchal plane: 0, concave; 1, flat; 2, convex.
102. External occipital protuberance: 0, concave; 1, convex; 2, flat.
103. Sagittal crest on supraoccipital: 0, absent; 1, present.
104. Massive elongation of supraoccipital: 0, absent; 1, present.
105. Anterior border of supraoccipital: 0, rounded; 1, borders converging and forming a sort of triangle in dorsal view.
106. Anterior border of supraoccipital in dorsal view: 0, narrow and rounded; 1, pointed; 2, narrow and squared; 3, wide and squared.
107. Lateral borders of supraoccipital: 0, uniformly convex; 1, uniformly concave; 2, straight; 3, sinusoidal.
108. Transverse constriction of supraoccipital: 0, moderate; 1, strong.
109. Lateral border of supraoccipital anterior to the strong constriction: 0, concave; 1, straight.

Exoccipital

110. Protrusion of posterolateral corner of exoccipital in ventral view: 0, absent; 1, strong and reaching a point posterior to occipital condyles; 2, strong and reaching a point anterior to occipital condyles.
111. Protrusion of posterolateral corner of exoccipital in ventral view: 0, largely medial to postglenoid process of squamosal; 1, posterior to postglenoid process of squamosal.
112. Occipital condyles: 0, show highly convex surfaces both dorsoventrally and transversely; 1, show convex surfaces only dorsoventrally and nearly flat surfaces transversely.
113. Occipital condyles: 0, with laterally concave neck; 1, with very short-to-absent, scarcely concave neck.

Basicranium

114. Infraorbital plate of maxilla: 0, absent; 1, present.
115. Location of optical channel: 0, under middle part of supraorbital region of frontal; 1, in posterior part of supraorbital process of frontal.
116. Basioccipital-basisphenoid suture obliterated by posterior termination of vomer: 0, no; 1, yes.
117. Palatine elongation: 0, palatine does not reach posterior border of skull; 1, palatine reaches posterior border of skull in ventral view.

118. Ventral lamina of pterygoid: 0, absent; 1, present.
119. Foramen pseudo-ovale: 0, absent; 1, present.
120. Foramen pseudo-ovale: 0, infundibulum incomplete; 1, infundibulum complete.
121. Location of foramen pseudo-ovale: 0, between squamosal and pterygoid; 1, within squamosal but with fissure towards pterygoid; 2, within pterygoid.
122. Posterior lacerate foramen: 0, absent; 1, present.
123. Posterior lacerate foramen located near to the posterior border of the skull: 0, no; 1, yes.
124. Anterior condyloid foramen: 0, present; 1, absent.

Periotic

125. Parabullary ridge in medial view: 0, highly convex dorsally; 1, mildly convex; 2, flat.
126. Maximum convexity of parabullary ridge located located over internal acoustic meatus in medial view: 0, yes; 1, no, it is more anterior.
127. Strong bulging of dorsal part of periotic: 0, absent; 1, present.
128. Endocranial opening of facial canal (adulthood): 0, located within internal acoustic meatus; 1, separated from internal acoustic meatus.
129. Endocranial opening of facial canal (later ontogeny): 0, located within internal acoustic meatus; 1, separated from internal acoustic meatus.
130. Endocranial opening of facial canal connected by a groove to the anterior rim of internal acoustic meatus: 0, no; 1, yes.
131. Endocranial opening of facial canal with fissure (adulthood): 0, no; 1, yes.
132. Endocranial opening of facial canal with fissure (later ontogeny): 0, no; 1, yes.
133. Suprameatal area gently descending towards internal acoustic meatus rim: 0, no, it is vertical; 1, strongly concave; 2, yes; 3, no, it protrudes.
134. Transverse elongation of pars cochlearis: 0, absent; 1, present.
135. Anteroposterior elongation of pars cochlearis: 0, absent; 1, present.
136. Anterior inflation of pars cochlearis: 0, present; 1, absent.
137. Median promontorial groove: 0, absent; 1, present.
138. Tensor tympani groove: 0, present; 1, absent.
139. Round window and perilymphatic duct confluent: 0, no; 1, yes.
140. Dorsal tuberosity of periotic cranially rounded: 0, no; 1, yes.
141. Anterior edge of pars cochlearis protruding cranially and forming a dorsoventral crest: 0, no; 1, yes.
142. Long and thick roof of stylomastoid fossa: 0, absent; 1, present.
143. Stylomastoid fossa: 0, broad and barely concave; 1, highly concave and forming a sort of notch at the emergence of posterior process.
144. Fossa for stapedial muscle well separated from round window by a thin crest: 0, yes; 1, no.
145. Anterior process of periotic: 0, absent; 1, present.
146. Anterior process of periotic: 0, long; 1, very short-to-nearly absent.
147. Anterior process of periotic in medial view: 0, blade-like; 1, thick.
148. Anterior process of periotic in dorsal view: 0, roughly round; 1, squared; 2, triangular.
149. Anterior process of periotic in dorsal view, triangular apex: 0, rounded; 1, pointed.
150. Anterior process of periotic in dorsal view, triangular and pointed apex: 0, medial border straight-to-slightly convex; 1, medial border concave.
151. Anterior process of periotic abruptly depressed from strong bulging of central part: 0, absent; 1, present.
152. Lateral process of anterior process of periotic: 0, absent; 1, present.
153. Lateral process of anterior process of periotic: 0, located at the emergence of the anterior process; 1, formed by the whole lateral edge of anterior process.
154. Lateral process of anterior process of periotic: 0, rounded; 1, triangular and short; 2, triangular and long.
155. Compound posterior process: 0, very short; 1, long.
156. Compound posterior process: 0, prismatic; 1, flattened.
157. Articulation between compound posterior process and squamosal: 0, tight; 1, weak.
158. Groove for facial nerve on posterior process: 0, long; 1, short.
159. Relative size of petrotympanic complex: 0, large; 1, very small; 2, small.

Tympanic bulla

160. Inner posterior prominence in dorsal view: 0, projects posteriorly; 1, does not project posteriorly.
161. Outer posterior prominence in dorsal view: 0, projects posteriorly; 1, does not project.
162. Posterior surface of tympanic bulla: 0, fissurated; 1, not fissurated.
163. Eustachian opening: 0, low; 1, high.
164. Dorsoventral height of tympanic cavity: 0, high; 1, low.
165. Interprominential notch in posterior view: 0, present; 1, absent.
166. Ventral surface of tympanic bulla: 0, highly concave; 1, convex; 2, keeled.
167. Anterolateral portion of tympanic bulla: 0, not

expanded (pyruliform bulla sensu Bisconti, 2010); 1, expanded.
168. Anterolateral expansion: 0, short; 1, long.
169. Anterolateral expansion: 0, continuous with anteromedial corner; 1, anteriorly separated from anteromedial corner by a lateral concavity visible in dorsal view.
170. Epitympanic hiatus: 0, small; 1, wide because of massive reduction of the height of conical process.
171. Dorsolateral border of involucrum in dorsal view: 0, straight; 1, concave; 2, convex.
172. Dorsal border of involucrum in medial view: 0, descending anteriorly; 1, projecting dorsally at anterior end.

Dentary
173. Teeth on dentary: 0, present; 1, absent.
174. Mental symphysis: 0, present; 1, absent.
175. Groove for mental ligament: 0, absent; 1, present.
176. Coronoid process: 0, high; 1, low; 2, absent.
177. Coronoid crest: 0, short; 1, long.
178. Position of coronoid process: 0, close to the condyle; 1, far from the condyle.
179. Postcoronoid crest and fossa: 0, absent; 1, present.
180. Postcoronoid fossa: 0, wide; 1, vestigial.
181. Satellite process: 0, absent; 1, present.
182. Satellite process: 0, high; 1, low.
183. Pterygoid fovea: 0, absent; 1, present.
184. Pterygoid fovea: 0, located medially; 1, located posteriorly.
185. Pterygoid fovea located posteriorly: 0, highly inclined; 1, scarcely inclined.
186. Protrusion of angular process: 0, absent; 1, ventral; 2, posterior.
187. Proportional size of angular process relative to the condyle in the dorsoventral plane (in lateral view): 0, angle larger than condyle; 1, angle half the size of the condyle; 2, angle severly reduced.
188. Condyle: 0, oriented dorsally and posteriorly; 1, oriented dorsally; 2, oriented posteriorly.
189. Articular surface of condyle in lateral view: 0, highly convex; 1, posteriorly flat.
190. Anterior torsion: 0, slight-to-absent; 1, strong.
191. Attach for mylohyoidal muscle: 0, apparently not developed; 1, sharp groove; 2, concavity; 3, crest.
192. Ventral border of dentary shows a lateral groove: 0, no; 1, yes.
193. Mandibular foramen: 0, wide; 1, small.
194. Mandibular foramen: 0, concave in medial view; 1, triangular.
195. Mental foramen: 0, bilateral foramens; 1, disintegrated into a series of foramens.
196. Gingival foramens and grooves: 0, absent; 1, present.
197. Dorsoventral arc of dentary ramus: 0, absent; 1, present in anterior-most portion; 2, present and continuous along the dentary.
198. Lateral arc of dentary ramus: 0, absent; 1, slight; 2, strong.

Vertebral column
199. Cervical vertebrae: 0, elongated; 1, very shortened.
200. Cervical vertebrae: 0, free; 1, fused.
201. Dorsal process in cervical vertebra No. 3: 0, present; 1, absent.
202. Dorsal process in cervical vertebra No. 4: 0, present; 1, absent.
203. Dorsal process in cervical vertebra No. 5: 0, present; 1, absent.
204. Dorsal process in cervical vertebra No. 6: 0, present; 1, absent.
205. Dorsal process in cervical vertebra No. 7: 0, present; 1, absent.
206. Ventral process in cervical vertebra No. 3: 0, present; 1, absent.
207. Ventral process in cervical vertebra No. 4: 0, present; 1, absent.
208. Ventral process in cervical vertebra No. 5: 0, present; 1, absent; 2, tubercle-like.
209. Ventral process in cervical vertebra No. 6: 0, present; 1, absent; 2, tubercle-like.
210. Ventral process in cervical vertebra No. 7: 0, present; 1, absent; 2, tubercle-like.
211. Foramen transversarium complete in cervical vertebra No. 3: 0, yes; 1, no.
212. Foramen transversarium complete in cervical vertebra No. 4: 0, yes; 1, no.
213. Foramen transversarium complete in cervical vertebra No. 5: 0, yes; 1, no.
214. Foramen transversarium complete in cervical vertebra No. 6: 0, yes; 1, no.
215. Foramen transversarium complete in cervical vertebra No. 7: 0, yes; 1, no.
216. Neural processes in cervical vertebrae: 0, free; 1, first-to-seventh cervical vertebrae have fused neural processes; 3, second-to-seventh vertebrae have fused neural processes.

Scapula
217. Inclination of cranial border: 0, scarce; 1, elevated;
218. Inclination of caudal border: 0, scarce; 1, elevated.
219. Supra-spinous fossa in lateral view: 0, present and wide; 1, present but reduced; 2, absent.
220. Infra-spinous fossa in lateral view: 0, concave; 1, flat.
221. Acromion process: 0, present; 1, absent.
222. Coracoid: 0, present; 1, absent.
223. Scapular spine: 0, present; 1, strongly reduced to absent.

Humerus
224. Forelimb proportions: 0, humerus has same length as radius and ulna; 1, humerus is shorter than radius and ulna; 2, humerus is longer than radius and ulna.
225. Medial tuberculum (deltopectoral crest): 0, present; 1, absent.

Radius
226. Radius and ulna can rotate at humeral articulation: 0, yes; 1, no.

Ulna
227. Olecranon process: 0, present; 1, absent.

Manus
228. Carpal bones in articulation: 0, yes; 1, no.
229. First digit: 0, present; 1, absent.
230. Fifth digit: 0, present; 1, absent.
231. Trapezium: 0, present; 1, absent.
232. Hyperphalangy: 0, no; 1, yes.

Hindlimb
233. Pelvis articulated with vertebral column: 0, yes; 1, no.
234. Functional hindlimb in adult: 0, yes; 1, no.

Ribs
235. Number of ribs that are articulated with sternum: 0, more than one pair; 1, one pair.
236. Rib 2: 0, bifid head; 1, single headed.
237. Rib 3: 0 bifid head; 1, single headed.
238. Rib 4: 0 bifid head; 1, single headed.
239. Rib 5: 0 bifid head; 1, single headed.
240. Rib 6: 0 bifid head; 1, single headed.
241. Rib 7: 0 bifid head; 1, single headed.
242. Rib 8: 0 bifid head; 1, single headed.
243. Rib 9: 0 bifid head; 1, single headed.
244. Rib 10: 0 bifid head; 1, single headed.
245. Rib 11: 0 bifid head; 1, single headed.

Sternum
246. Sternum formed by several sternebra: 0, yes; 1, no, it is formed by manubrium only.

Appendix 2: Matrix used in cladistic analysis

Protocetus atavus Fraas, 1904
0-000--0- 0000-0---- ------0000 0000000000 0000000000 0000000000 0-?000-000 0100000-0- 0---000100 000000??00 -00000-0-- 0000001001 ?0101????? ????000??0 ????1?????? ????000000 0000000--- -10??????? ?????????? ?????????0 000?000000 000000000? ?????????? ?????????? ???????

Georgiacetus vogtlensis Hulbert et al., 1996
0-000--0- 0000-0---- ------0000 0010000010 0000000000 0000000000 0-0000-000 0100000-0- 0---000000 0000000000 -00000-0-- 0000000001 10100????? ????000??0 ?????1???? ?????000?0 00000000-- -100000-00 -0-0--0000 0000010000 0?00?0?00? 0?00?00??? ?????????? ???00?0000 000000?

Dorudon atrox Andrews, 1906
0-000--0- 0000-0---- ------0000 0010000010 0000000000 0000000000 0-0000-000 0000000-0- 0---000100 0000000000 -00100-0-- 0000000001 1010100000 0000000100 -0000100?- -00--00010 00000000-- 0000000-00 -0-0--0000 0000010000 0000000000 0000000000 0000000000 0001000000 0000110

Zygorhyza kochii Reichenbach in Carus, 1847
0-000--0- 0000-10111 0110000000 0010000010 0330010000 2000010000 0-0000-000 000001010- 0---000100 0000000000 -01000-0-- 0000001001 1010000000 0000000000 000000101?? ?????000?0 00000000-- 0000000000 -0-0--0000 0000010000 00??0?0??0 00??000000 00000000?? ???11?0000 0001110

Mammalodon colliveri Pritchard, 1939
100?0--11 1000-10101 1-0000?011 00??010?20 00?2000000 0000?00000 0-?000-000 0100000-0- 0---??0?0? ????????00 -01100-0-- 0?0010???1 1010000000 0000100000 000001011- -00--????0 00000000-- 0100000-00 -0-0--0200 000001000? 0????????? ?????????? ?????????? ?????????? ??????0

Aetiocetus weltoni Barnes et al., 1995
00000--11 1011111111 0100001101 00001-0120 0001010000 0000100010 0-0000-001 110001010- 0---100100 100011000? ????0????? 0000100001 11101????? ????????00 ???0?1?1?? ?????1?000 00000000-- 0100110-00 -0-0--0100 000001000? ?????????? ?????????? ?????????? ?????????? ???????

Eomysticetus whitmorei Sanders, Barnes, 2002b
1???0--?? ??1110---- ------11?? 00101-1110 00010?1010 0000000012 0-?000-000 010000010- 0---100010 002001??01 00110112-- 1111?01001 101010001? 0001000000 0000?1001- -00--00111 00000000-- 0001110-00 -0-0--0100 0000011001 000?0000?0 0???1101?? 001?0010?? ??????0000 000111?

Micromysticetus rothauseni Sanders, Barnes, 2002a
????????? ?????????? ?????????? ?????????? ?????????? ??????0??? ???100-001 110000010- 0---100110 002001??01 00110100-- 1011??1001 101010000? 0001000000 0000?1001- -00--00011 ?????????? ?????????? ?????????? ?????????? ?????????? ?????????? ?????????? ???????

Caperea marginata Gray, 1846
000011010 101100---- ------1111 00101-1120 0022002011 2210121122 0-13---102 210101010- 1022111102 0010040210 -21110-0-- 1111101011 121111001? 0002000110 010001002? ?????10000 1110110100 1201112--0 -0-10-0110 0101011201 1000001111 1111111112 0000111010 1111110000 0011111

Balaenula astensis Trevisan, 1941
211011010 10?100---- ------0111 00101-1120 00020?1021 0110121122 0-?3---002 210000000- 0---111102 001004??10 -21010-0-- 2011101110 0011020??? ???000??0? 0010?1011- -011?10100 1111110100 1201112--0 -0-10-0110 1101011201 1000000000 0111112001 1011111110 0111110000 0000011

Eubalaena glacialis Müller, 1776
211011112 101100---- ------0111 00101-1120 0002001021 0110121122 0-13---112 210000000- 0---101102 0010130110 -21010-0-- 2011101110 1011100000 0003100100 011011011- -011110100 1111110100 12011120-0 -0-10-0110 1101011221 1000000000 0111112001 1011111110 0111110000 0000011

Balaena mysticetus Linnaeus, 1758
211011012 101100---- ------0111 00101-1120 0002001021 2210121122 0-13---112 210000010- 0---101102 1020130110 -2101123-- 2011101111 0011100000 0000000100 001001011- -010210000 1210110100 12011120-0 -0-10-0110 1101011221 1000000001 2111112001 0011111110 0111111000 0000011

Balaenella brachyrhynus Bisconti, 2005
000011012 101100---- ------0111 00101-1121 0222001021 2210121122 0-?3---112 210000010- 0---101102 0020130110 -1101123-- 201110?011 00111????? ????000100 ?010?1011- -011210000 1110110100 120??????? ?????????? ?????????? ?????????? ?????????? ?????????? ?????????? ???????

Pelocetus calvertensis Kellogg, 1965
20110--10 101110---- ------1111 00101-1120 11?2001020 1130120132 0-?100-001 110100000- 0---100110 0020000210 -0000112-- 1011101001 111010000? 0000000100 000101010- -012010000 1110011110 0101??1011 00-10-1120 0000011021 000?0000?0 011?110100 0100211??? ?????10000 000011?

"Aglaocetus" patulus Kellogg, 1965c
20110--10 101110---- ------1111 00101-1120 11?2001020 0210120132 0-?100-001 110000000- 0---100100 0020000210 -0000112-- 2011101001 111010000? 00?0000100 000001010- -012010000 1110011110 010??????? ??-??????? ?????????1 00?0??0?0? ?1?1??0??? ?????????? ?????????? ???????

Isanacetus laticephalus Kimura, Ozawa, 2002
20110--10 1011110001 ?-----1111 00101-1120 11?2011020 1210120132 0-?100-001 110100010- 0---100100 0020021-10 -0010112-- 2011101001 1010100000? 00?0000100 0000?10120 -010010000 1010011110 010111???? ??-??????? ?00??11??1 00??0?0??1 ?1??1?0??? ?????????? ?????????? ???????

Uranocetus gramensis Steeman, 2009
20110--10 101110---- ------1111 00111-1120 1112001020 011??20132 0-?10?-001 110100010- 0---1001?0 0?2002??10 -0?10113-- 201110100? ??101???0? 00??000100 ?00001 0?0- -0???????0 1110011110 0101??1??? ?0-????1120 0000011 0?1 000???00?? ?00???0000 0000111 0?? ?????10??? ??????1

Parietobalaena palmeri Kellogg, 1924
20110--11 101110---- ------1111 00111-1120 1112001020 1110120132 0-?100-001 110000010- 0---100100 0120040211 0011011300 1111001001 111010001? 10?0000100 000101100- -010010100 11100110-- 0001111011 00-10-1120 0001011011 00000?0000 ??????0??? ?????????? ?????????? ???????

Aglaocetus moreni Kellogg, 1934b
20110--11 1011110101 0000001111 000111-112 0032001020 0110130112 0-?1010001 110100010- 0---100100 0020040110 -0000113-- 1111101001 11101????? ????000??? ?????????? ?????1010? ?????????? ???1111011 00-10-1120 0001011102? ?????????? ?????????? ?????????? ?????????? ???????

Titanocetus sammarinensis (Capellini, 1901)
20110--11 0011110101 0022000111 0010001120 0332001020 1130130112 0-?1010002 210110010- 0---100100 00200?0100 -00000-0-- 2011101100? ??101????? ?????????? ?????????? ?????101?? ?????????? ???1111011 ?0-0--0121 0001111021 00????0??? ??????0??? ?????????? ?????????? ???????

Cophocetus oregonensis Kellogg, 1934a
20110--10 1111110001 1-00001111 00111-1120 0002001020 1130110112 0-?1010001 210100010- 0---100100 00100?0110 -0000113-- 1011101001 11101???0? 00?0000100 ?0??0101?? ?????1010? 1110011110 0001??1011 00-10-1120 0000111011 0??00?0000 1?????0001 0000111010 0?111????? ???????

Diorocetus hiatus Kellogg, 1968b
21110--10 1011110001 1-00001111 00111-1120 1002001020 1110120112 0-?100-001 210100010- 0---100100 0120040211 0001011300 2011101001 111010101? 10?0000100 000?010120 -00--10100 11100110-- 0101111011 00-10-2120 0001011011 0???00???1 1?????011? ?000??10?? ?????????? ???????

Joumocetus shimizui Kimura, Hasegawa, 2010
20?10--?? ??1110---- ------1111 00111-1120 11320?10?? 021??20132 0-?100-001 2100?0010- 0---??0??? ?????????0 -001011300 1?11101??? ??101????? ????0110?0 ?0???100?? ?????000?0 111??110-- ?10111???? ??????2121 000??1101? ?????????? ?????????? ?????????? ?????????? ???????

Cetotherium rathkii Brandt, 1873
?11?0--11 1111111001 1-10001111 00??001?20 1112001010 1110130112 1-?2011001 21010001?? ????100100 001002??01 0011010100 1111101001 1?101????? ?????????? ?????????? ?????????0 11100110-- 0?01?????? ?????????? 000??1101? ?????????? ?????????? ?????????? ?????????? ???????

Piscobalaena nana Pilleri, Siber, 1989
21100--11 1111111001 1-11001111 0011001130 1112001010 1110130100 1-11011001 210100110- 0---100100 0120041-00 -001010000 1111111001 1110111011 1000000100 100101010- -010000100 12100110-- 0101111011 00-10-2100 0001011021 0000000000 1001110111 000011101? ???1110000 0011111

Mixocetus elysius Kellogg, 1934c
21100--11 1111111001 1-00001111 00111-1130 0102001010 1110130012 1-?1011001 21011011?? ????100100 0?10??01?? ?????????? 1111111001 11101????? ????000??? ????1????? ?????1000? ?????????? ???1111110 00-?????20 0001?11??1 0000000000 00????0111 0000?????? ?????????? ???????

Metopocetus durinasus Cope, 1886
????????? ?????1100? 1-1100???? ????01???0 11???????? ?????30?12 1-?1011001 210?101?0- 0---??010? ?????????1 0001010300 ??????1??? ?????1101? 10?0000100 100??101?? ?????????? ?????????? ?????????? ?????????? ?????????? ?????????? ?????????? ?????????? ???????

"Cetotherium" megalophysum
21100--10 101110---- ------1111 00101-1120 1102001010 1110120132 0-?100-001 210010010- 0---000100 001004??00 -000011300 1111111001 10101????? ?????????? ?????????? ?0???10100 111??110-- ???1111011 00-10-0120 000101101? ?????????? ?????????? ?????????? ?????????? ???????

Eschrichtius robustus (Lilljeborg, 1861)
211010011 1111111111 0100011111 00101-1120 0012002011 2220030010 1011011001 210011110- 100?100101 0010020101 1210002300 1111111001 101010100? 00?1110101 0100?10120 -00--11100 1111011110 0201112-1- -1110-2110 0201011211 0000000000 0111110002 0000111010 1111111000 0011111

Eschrichtioides gastaldii (Portis, 1885)
2???0--?? ??11111101 0100001111 001?001120 0012002011 012?130010 1011011001 211011010- 101?100101 002012??01 112000-0-- 11111?1001 10101????? ?????????? ?????????? ?????110?0 1111011110 0001111011 -1110-1110 0201011221 0????????? ?????????? ????1110?? ???11????? ???????

Archaeschrichtius ruggieroi Bisconti, Varola, 2006
????????? ?????????? ?????????? ?????????? ?????????? ?????????? ?????????? ?????????? ?????????? ?????????? ?????????? ?????????? ?????????? ?????????? ?????????? ?????????? ???1110011 010??????? 000??1122? ?????????? ?????????? ?????????? ?????????? ???????

Archaebalaenoptera castriarquati Bisconti, 2007a
20100--10 1011111101 0100011111 0011001120 0001002121 2231130011 10?2012102 2111011010 ????100100 003013??11 0011010310 1???1????? ????1????? ?????????? ?????????? ?????110?0 ?????????? ???111???? ?????????0 ?????1101? ?????????? ?????????? ?????????? ?????????? ???????

Parabalaenoptera baulinensis Zeigler *et al*., 1997
20??0--?? ??11111111 0100011111 00101-1120 1031002120 2230131011 10?3012112 210001100- ????100100 001002??10 -1?00122-- 01111?1001 10101????? ?????????? ?????????? ?????110?0 111101???? ???1111110 10-11?0?21 00?1011021 00????0??? ?0????0??? ?????11??? ?????????? ???????

Megaptera novaeangliae Brisson, 1762
20110--12 1011111100 0100001111 0010001141 0002102121 2231130011 1112012112 211001100- 1121100001 0030001-10 -121010300 0011111001 1010111100? 0001110000 0101110120 0010111110 1110011110 0201112-10 ?0-1110221 0011011021 0000000002 1111110112 0111111010 1111111001 1111111

Balaenoptera physalus Linnaeus, 1758
20110--10 1011111121 0100001111 00101-1141 0002002121 2231130012 1112012112 2110011010 1121100000 1010110110 -100013300 2011111001 1010111011 0012110010 0000110121 0010111110 1111012111 0211111011 10-1110221 0011011021 0000000000 2000110111 0000111010 1111110011 1111111

Balaenoptera acutorostrata Lacepede, 1804
01110--10 1011111121 0100001111 00101-1130 0122002121 2231130011 1112012112 2110011111 1121000000 1010110110 -120013300 0011111001 1011121001 0011111100 0001110121 1010111110 1111012111 0211111011 10-1110221 0011011021 0000000002 1001110112 0000111010 1111111000 0111111

Balaenoptera edeni Anderson, 1879
20110--10 1011111121 0100001111 00101-1130
0112002121 2011130011 1112012112 211001110-
112?100000 1010110110 -100013300 0011111001
101012-001 0013110010 0101110121 0010111110
1111012111 0211111011 10-1110221 0011111021
000000???? ???????112 0000111010 111111???? ??????1

Balaenoptera borealis Lesson, 1828
20110--10 1011111121 0100001111 00101-1130
0112002121 2231130011 1112012112 2110011011
112?100000 1010110210 -100013300 0011111001
101012-001 0013111011 0100110121 1010111110
1111012111 0211111011 10-1110221 0011011021
000000???? ???????112 0000111010 111111???? ??????1

Balaenoptera musculus Linnaeus, 1758
20110--10 1011111121 0100101111 00101-1130
0012002121 2231131011 1113---112 210001100-
1102100000 1030110111 0120013300 0011111001
11101??1?? ????110001 ??00?10121 0110111110
1111012111 0211111111 10-1110221 0011011021
0000000000 1000110111 0000111010 1111110000
0111111

"Balaenoptera" siberi Pilleri, 1989
20110--10 1011111121 0100101111 00101-1141
0002102121 2230131011 1110112102 210001110-
????100100 003000??10 -01000-0-- 10111?1??1
????1????? ?????????? ?????????? ?????????? ??????????
???111???? ?????????? 0????11021 0?????????
???????111 0000111010 111111???? ??????1

new taxon #2 (Peru)
20110--10 1011111111 0100001111 00101-1140
0001102121 2231130011 10?2012112 2110010110
11111?1000 0031110011 00210122-- 1111111001
11101????? ?????????? ?????????? ?????110?2
111?012111 ?????????? ?????????? ?????????? ??????????
?????????? ?????????? ?????????? ???????

"Plesiocetus" cortesii var. *portisi* Sacco, 1909
20110--?? ??111111?0 01??001111 11100-11?? ??????2121
2230120011 10?1010111 111001000- 110?100100
0031140111 0220011311 1111111001 ??101?????
????111??? ?????????? ?????110?2 1110012???
?101111011 00-1102221 0001011011 0000000000
0?????0112 0000?????? ?????????? ???????

Protororqualus cuvieri Bisconti, 2007b
20110--11 0111111101 0100011111 10101-1130
0112002120 2230130011 10?2012111 111001100-
????100100 ??30????11 0001011311 1011111001
10101????? ?????????? ?????????? ??????????
111?012??? ?2?1111011 00-???0221 00?1011011
00????0??? ??????0112 00001110?? ??1111?001 1111111

Plesiobalaenoptera quarantellii, Bisconti, 2010
20110--11 101111110? 01?0011111 0011??11??
??????212? 2??????0?1 ?0?????11? ????0???1?
????1????? ?????????0 -000012??? ??111?????
????10111? 10?1111100 0000010120 0110011?10
1111012110 0211111010 00-1110221 0200011021
000???00?? ?00????0??? ?????????? ?????????? ??????1

New taxon #3 (Peru)
20110--10 1011111101 0100001111 0010011140
0001102121 2231130011 1012012102 2111011010
11??100100 003001??11 001001030- 1?11??????
?????????? ?????????? ?????????? ?????????? ??????????
???111???? ????1110221 ???1011??1 000000????
??????0??? ?????????? ?????????? ???????

New taxon #1 (Italy)
20??0--?? ??11111121 0100001?11 0010??1130
0001002121 2230130011 10?2012112 2110011111
110?100101 0030011301 0010012311 1011111?01
10101????? ????110?0? ?0???10121 0?10001000
1????????? ?????????? ?????????? ?????????1
0000000011 ?1111?0??? ?????????? ?????????? ???????

"Megaptera" hubachi Dathe, 1983
20110--?? ??11111101 0100001111 00111-1140
0100102121 2231130011 10?2012112 2110011??
110?100100 003000??10 -00001230- 1011111001
11101???1? ????1100?1 ?????10121 0????????0
?????????? ???1111011 00-1110121 0011011021
0000000000 1111110111 0000111010 1111110000 0111111

Diunatans luctoretemergo Bosselaers, Post, 2010
????????? ??111111121 ??0000??1? ????1-1141
0002102l?? ?????30011 11?2112112 2110011???
111?100101 0010010010 -01001330- 1011??1001
101012-01? 00?1110100 00?1010121 0-10111?0
1111012??? ?11???????? ?????????? ?????????1
000???00?? ?????????? ?????????? ?????????? ???????

Riassunto

Lo studio dell'olotipo di "Megaptera" hubachi ha rivelato che questo reperto non può essere assegnato al genere Megaptera. Caratteristiche-chiave di Megaptera comprendono infatti un processo postglenoideo dello squamoso che proietta nettamente in basso, un processo sovraorbitario del frontale che proietta nettamente indietro, processi ascendenti del mascellare the terminano anteriormente all'orbita, assenza di processo coronoideo della mandibola e delle strutture ad esso associate. In "Megaptera" hubachi il processo postglenoideo proietta leggermente più in basso del processo zigomatico dello squamoso e la cavità glenoidea è solo leggermente concava; il processo coronoideo della mandibola è presente con tutto il suo complemento di cresta e fossa postcoronoidea; i processi ascendenti del mascellare sono lunghi e il processo sovraorbitario del frontale non proietta posteriormente. L'analisi comparata e lo studio filogenetico suggeriscono quindi la necessità di coniare un nuovo nome generico per questo reperto.

L'analisi filogenetica è stata eseguita attraverso uno studio cladistico di una matrice con 244 caratteri osteologici e 2 caratteri dei fanoni codificati per 50 taxa. I risultati rappresentano uno dei più vasti studi filogenetici focalizzati sui Mysticeti. Lo studio supporta il monofiletismo di Balaenopteridae il cui sister group è Eschrichtiidae. La definizione entro Balaenopteridae è bassa ma lascia intravedere la possibilità di esistenza di almeno tre sottofamiglie da definire una volta che il loro supporto morfologico sia stato incrementato. Le caratteristiche morfologiche dei distretti cranici legati al comportamento alimentare di "Megaptera" hubachi mostrano alcune differenze con i balenotteridi moderni. Tra queste, l'assenza di una cavità glenoidea dello squamoso particolarmente concava, la presenza di fossa postcoronoidea e un bordo ventrale della mandibola non particolarmente acuto suggeriscono che i meccanismi responsabili dell'intermittent ram feeding the balenotteridi non fossero ancora in posto in questo reperto. E' necessario un aumento della risoluzione dei rapporti filogenetici entro Balaenopteridae per delineare il percorso o i percorsi evolutivi dei meccanismi alimentari specializzati dei balenotteridi che al momento non possono essere ricostruiti con certezza.

How to cite this paper:
Bisconti M., 2010. New description of "*Megaptera*" *hubachii* Dathe, 1983 based on the holotype skeleton held in the Museum fur Naturkunde, Berlin. In Bisconti M., Roselli A., Borzatti de Loewenstern A. (eds.), Climatic change, Biodiversity, Evolution: Natural History Museum and Scientific Research. Proceedings of the meeting. Quad. Mus. St. Nat. Livorno, 23: 37-68.